The Mineral Exploration-Mineral Deposits and Tectonics of two Contrasting Geologic Environments in The Republic of the Philippines

Consolidated Report on The Palawan Area

Contents

List of Figures

List of Tables

List of Attached Plates

PL-1-1 Northern Palawan Geological Map and Section (1/1,000,000)

PL-1-2 Southern Palawan Geological Map and Section (1/1,000,000)

PL-2-1-1 (No. 1 to No. 12) Northern Palawan Geochemical Analysis Cell Average Values Distribution Map (1/1,000,000)

PL-2-1-2 (No. 1 to No. 9) Southern Palawan Geochemical Analysis Cell Average Values Distribution Map (1/1,000,000)

PL-2-2-1 (No. 1 to No. 12) Northern Palawan Geochemical Analysis Moving Average Values Distribution Map (1/1,000,000)

PL-2-2-2 (No. 1 to No. 9) Southern Palawan Geochemical Analysis Moving Average Values Distribution Map (1/1,000,000)

PL-2-3-1 (No. 1 to No. 12) Northern Palawan Geochemical Analysis High-pass Filter Values Distribution Map (1/1,000,000)

PL-2-3-2 (No. 1 to No. 9) Southern Palawan Geochemical Analysis High-pass Filter Values Distribution Map (1/1,000,000)

PL-2-4-1 (No. 1 to No. 5) Northern Palawan Geochemical Analysis Factor Values Distribution Map (1/1,000,000)

PL-2-4-2 (No. 1 to No. 4) Southern Palawan Geochemical Analysis Factor Values Distribution Map (1/1,000,000)

PL-3-1 Northern Palawan Distribution Map of Anomalous Values in Panned Samples (1/1,000,000)

PL-3-2 Southern Palawan Distribution Map of Anomalous Values in Panned Samples (1/1,000,000)

PL-4-1 Northern Palawan Distribution Map of the Major Heavy Wt. % in Panned Samples (1/1,000,000)

PL-4-2 Southern Palawan Distribution Map of the Major Heavy Wt. % in Panned Samples (1/1,000,000)

PL-5-2 Southern Palawan Compiled Gravimetric Map (Bouguer Anomalies) (1/1,000,000)

PL-6-1 Northern Palawan Compiled Aeromagnetic Map (1/1,000,000)

PL-6-2 Southern Palawan Compiled Aeromagnetic Map (1/1,000,000)

PL-7-1 Northern Palawan Lineaments Map (LANDSAT Images) (1/1,000,000)

PL-7-2 Southern Palawan Lineaments Map (LANDSAT Images) (1/1,000,000)

PL-8-1 Northern Palawan Locality Map of Mineral Showings (1/1,000,000)
Attached Index Table of Mineral Showings

PL-8-2 Southern Palawan Locality Map of Mineral Showings (1/1,000,000)
Attached Index Table of Mineral Showings

PL-9-2 Southern Palawan Index Map of Existing Data regarding Survey Works of the Area (1/1,000,000)

PL-10-1 Northern Palawan Relation Map between Promising Area and Mineral Showings Localities (1/1,000,000)

PL-10-2 Southern Palawan Relation Map between Promising Area and Mineral Showings Localities (1/1,000,000)

Appendixes

Appendix 1 Histograms and Cumulative Frequency Curves of Cell Average Values

Appendix 2 Flow Charts of Chemical Analysis

Appendix 3 Existing Data List

1. Introduction

1-1 Purpose and Scope

1-1-1 Background and Particulars

Pursuant to the Implementing Arrangement (I/A) entered into between the Government of the Philippines through the Mines and Geo-Sciences Bureau (MGB) and the Government of Japan through the Japan International Cooperation Agency (JICA) and the Metal Mining Agency of Japan (MMAJ) signed on Sept. 26, 1984, a project officially titled Mineral Exploration-Mineral Deposits and Tectonics of Two Contrasting Geologic Environments was carried out in the Republic of the philippines.

This report embodies the results of the synthetic evaluation of the Palawan Area which is included in the above mentioned exploration project. The field survey took place from January to February in 1986, and January to March in 1987 (JICA-MMAJ Report, 1987; 1988).

1-1-2 Objectives of the Report

This report embodies the summary of the results of the survey results and existing data regarding the mineral resources in the Palawan Area which is located in the western part of the Republic of the Philippines.

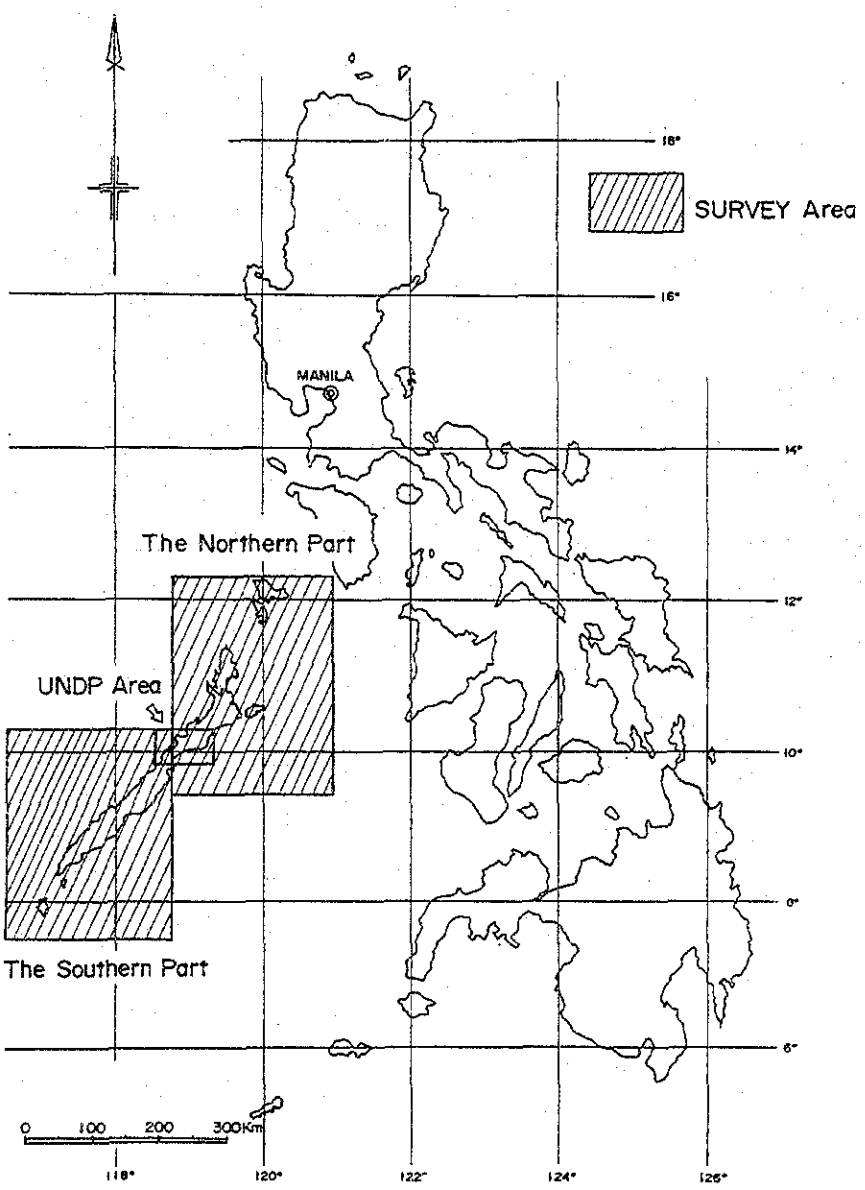

Fig. 1 Location Map of the Survey Area

The objectives of this report include the recognition and derivation of the mineral resources distribution in the different survey areas, correlating, processing and analyzing all acquired data and the synthetic evaluation of the area.

1-2 Regional Setting (Ref. Figs. 1 and 3)

1-2-1 Location and Accessibility

1-2-1-1 Location

The Palawan Area is located in the westernmost portion of the Republic of the Philippines, and belongs to Region IV.

This area is composed of the Calamian Group (consisting of the Busuanga Island, Coron Island, Culion Island and Linapacan Island), and main Palawan Island and Balabac Island. The total survey extent is 10,520 km^2.

1-2-1-2 Accessibility

There is a regular flight daily from Manila to Puerto Princesa. Ship services plying the Manila to Puerto Princesa rout are available twice a week. Only few of the inland roads in the island are paved at the moment.

1-2-2 Climate and Vegetation

The Palawan area belongs to the Western Pacific Monsoon Climatic Zone. The dry season (December to May in the main Palawan Island and January to July in the Calamian Group) and the rainy season (June to November in the main Palawan Island and August to December in the Calamian Group) are distinctly observable.

Annual precipitation is 2,000 mm in the northern part and 2,200 mm in the southern part. Average temperature is 27°C degree.

The inland portions of the Palawan Islands Group are usually covered by virgin forests. However, the mountain ranges of the Calamian islands are deforested due to the extensive logging in the area.

The alluvial plains along the rivers and coastal regions are planted with rice, coconut and banana.

1-3 Personnel Involved

1-3-1 Planning and Negotiation

Japanese Panel:

Takeshi Izumi	Metal Mining Agency of Japan (MMAJ)
Kyoichi Koyama	id
Hideo Hirano	id

Natsumi Kamiya	Metal Mining Agency of Japan (MMAJ)
Yoshitaka Hosoi	id

Philippine Panel:

L. T. Abuyuan	Department of Environment and Natural Resources (DENR)
G. R. Balce	Mines and Geo-Sciences Bureau (MGB)
R. M. Luis	id
E. G. Domingo	id
R. L. Almeda	id
N. V. Ferrer	id

1-3-2 Preparation of the Consolidated Report

Japanese Panel:

Yoshikazu Okubo	Overseas Mineral Resources Development Co. (OMRD)
Yukio Uehara	id
Yoshihiko Shimazaki	id
Akio Shida	Nittetsu Mining Consultants Co., Ltd.
Kazuyoshi Masubuchi	Dowa Engineering Co., Ltd.

Philippine Panel:

R. M. Samaniego	Mines and Geo-Sciences Bureau (MGB)
M. V. Garcia	id
B. S. Vargas	id
R.M. Luis	id
R. L. Almeda	id
R. Villones	id
A. Apostol Jr.	id
M. A. Aurelio	id
R. A. Santos	id

1-4 Methodology

The analysis and interpretation of the geoscientific data from the Palawan area were conducted as follows:

1-4-1 Survey area (Ref. Fig. 1)

The survey area is divided by Sabang thrust for convenience of geological description and geochemical analysis, into a northern part (hereafter called the Northern Part) and southern part (hereafter called the Southern Part).

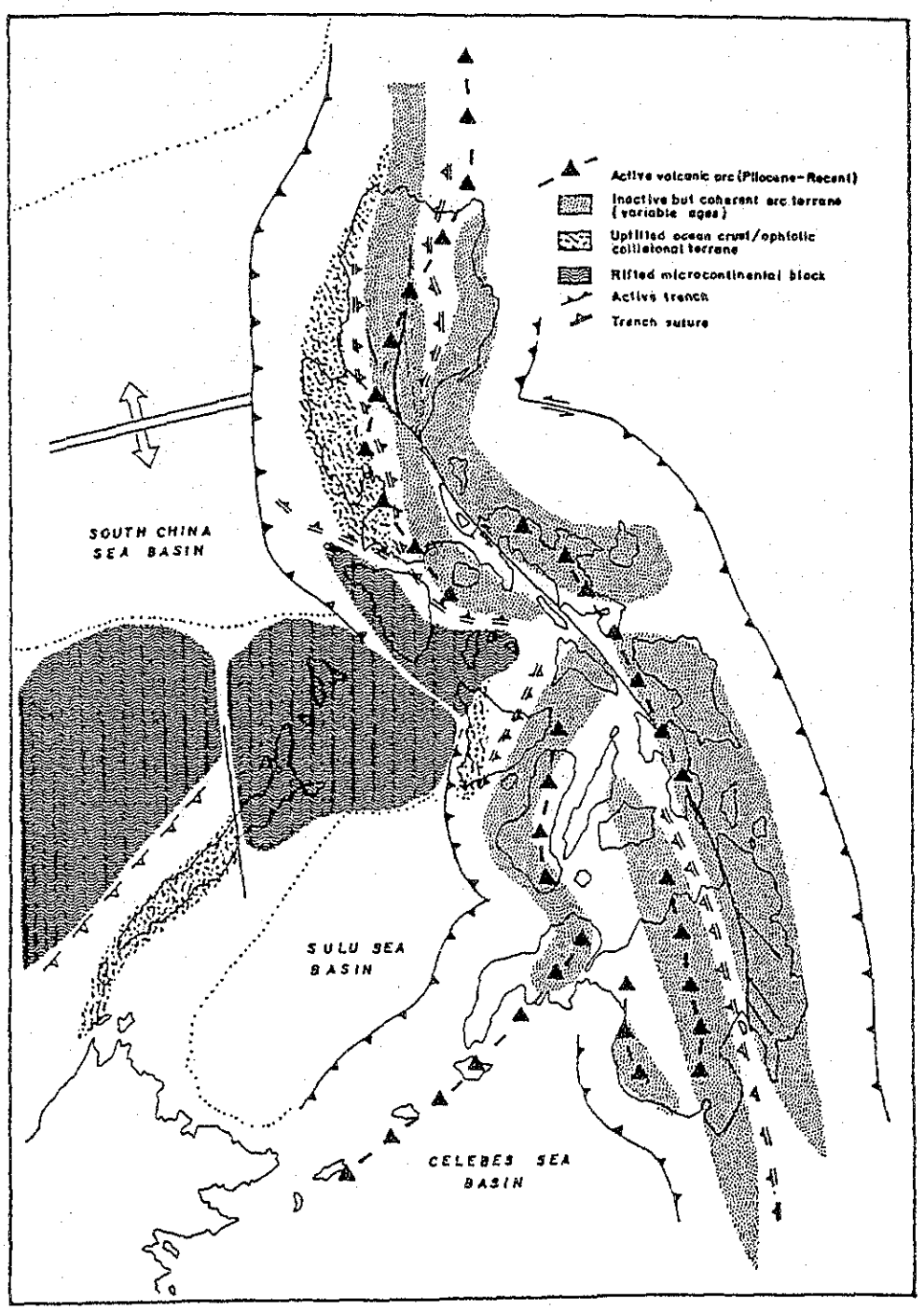

Fig. 2 Tectonic Terrans of the Philippinea (After A. S. Zanoria et al. 1984)

1-4-2 Stratigraphy (Ref. Figs. 4, 5)

In this report the stratigraphic classification which had been agreed upon between the Japanese and Philippine panels during the workshop held in Manila in June, 1988 was used.

A geological map in the scale of 1:1,000,000 has been prepared in conformity with the stratigraphic classification.

1-4-3 Geochemical Data

In terms of the geochemical data, the zones with anomalous values were identified utilizing the following processes.

The whole survey area is divided into 2 km × 2 km cells. The univariate and multivariate analyses of the average values of all the cells were carried out. The univariate analyses of the moving average values of all cells and of the high-pass filter values were also made. The high-pass filter values were calculated from the difference between the cell average and the moving average values.

A total of 8,426 stream sediment samples including 2,250 samples by UNDP., 1985 (grain size less than 0.175 mm) were used in these analyses. The details of the samples and analyzed elements are as follows:
collected and analyzed for 14 elements (Cu, Pb, Zn, Ag, As, Mn, Ni, Co, Mo, Hg, Cr, Sb, Sn and W)

In the Southern Part, 4,207 stream sediments samples were collected and were analyzed for 10 elements (Cu, Pb, Zn, Ag, As, Mn, Ni, Co, Hg and Cr)

1-4-4 Data of Heavy Mineral Samples

In addition to these samples, a total of 413 (177 in the Northern Part and 236 in the Southern Part) heavy mineral samples were collected by panning. Au, Ag, and Ga analyses were conducted and the analytical data were processed by univariate analysis.

Fifty of the above samples, twenty (20) from the Northern Part and thirty (30) from the Southern Part were selected at random and the mode of component minerals of these samples were analyzed.

1-4-5 Existing Data

Available existing data were compiled in a lineament map, in an aeromagnetic map, in a gravity map and in a data index map. These were compiled in 1:1,000,000 scale to conform with the geologic, geochemical and other maps of this project. Most of these maps are printed in color.

The localities of previous geo-scientific works of the area are shown in PL-9-1 and PL -9-2 and list of their works are attached in Appendix 3.

1-5 Achievements of the Project

1-5-1 Conclusions

The mineralization is significantly different between the Northern and the Southern Part. In the Northern Part, of the sedimentary manganese mineralizations, of the disseminated chromite associated with ultramafic rocks and stibnite bearing quartz veins are observed sporadically.

On the other hand, the Southern Part is characterized by the existence of extensive Ni-laterite and chromite deposits associated with ultramafic rocks, Cyprus type massive sulfide copper deposits and hydrothermal veins associated with Cretaceous basalts, and mercury deposits located in the basement window at the northern portion of Puerto Princesa.

The following six promising areas for further exploration were delineated on the basis of the mineral showings and the results of the geochemical surveys conducted.

The target commodities are indicated for each respective areas.

(A) The southern part of Pulute Range in the Southern Part. (Expected commodity: Ni and Cr)

(B) The northern mountain zone of Barong-Barong in the Southern Part. (Expected commodity: Cu and Zn)

(C) The southward portion of the Moorsom Point at the west coast in the Southern Part. (Expected commodity: Ni and Cr)

(D) The area of basement window exposure north of Puerto Princesa in the Southern Part. (Expected commodity: Hg, Cu and Mn)

(E) The northwestern part of Tinitian at the southern coast on the Northern Part. (Expected commodity: As and Sb)

(F) The vicinity of El Nido to Mt. Kapoas in the Northern Part. (Expected commodity: Cu, Zn and Sn)

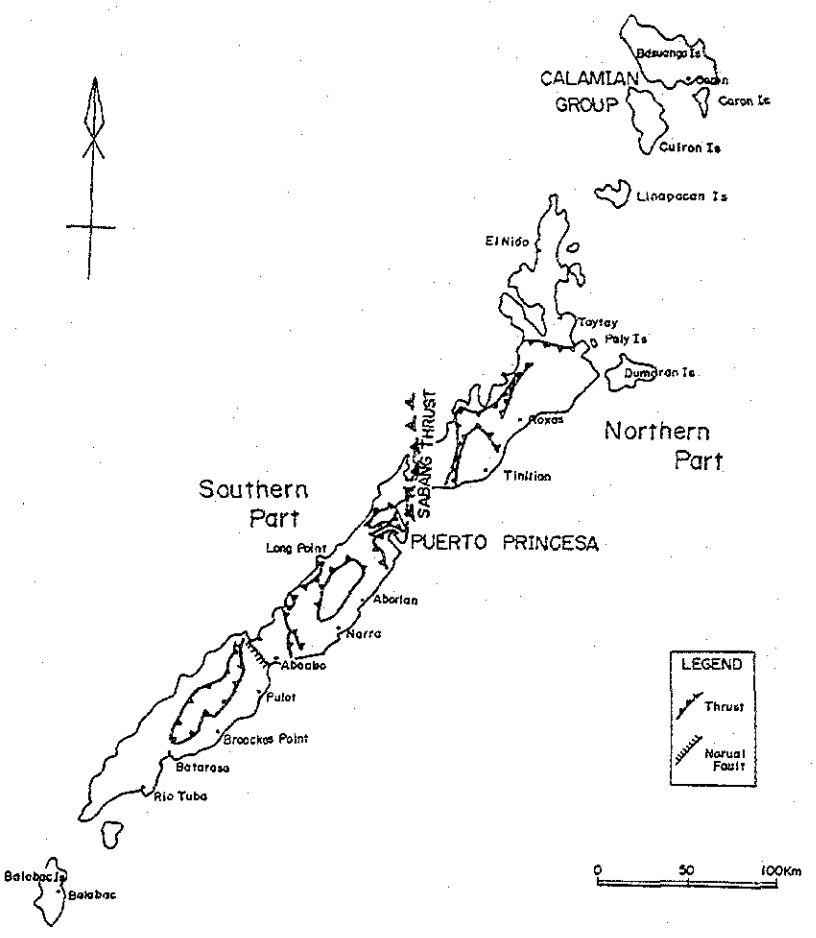

Fig. 3 Tectonic Division Map of the Palawan Area

2. Geology and Mineralization of the Area

2-1 Geological Setting (Ref, Figs. 2, 3 and Attached Plate-1)

2-1-1 Regional Geology

The survey area is located at the western part of the Philippine Archipelago and belongs to the Palawan Physiographic Province, and forms the stable uplifted block.

The area is divided into the northern Palawan and the southern Palawan by the Sabang Thrust which passes at central part of the main Palawan Island at a low angle.

The Northern Part consists mainly of pre-Cretaceous sedimentary and meta-sedimentary rocks, while the Souther Part is composes of 'Cretaceous to Oligocene basal rock unit, both sedimentary and basaltic rocks and ultramafic rocks thrusted over these basement.

2-1-1-1 The Northern Part

The northern parts of the main Palawan Island and the Calamian Group are composed of uplifted basement chert and limestone which constitute in part.

The igneous bodies in the Northern Part are the Kapoas Diorite intruded at the Kapoas Peninsula and at east side of the Ulugan bay during the Oligocene time and the Manguao Vocanics exposed at the eastern side of the northern main Palawan Island in the Pleistocene time.

In the northern central part of the main Palawan Island, the basement consists of phyllitic rocks and mica shcist. These basement rocks are covered by Tertiary sedimentary rocks and thrusted over by the ultramafic rocks at Paly Island offshore east of the main Palawan Island.

The geologic structures of the basement rocks suggest the strong deformation it had undergone in connection with its collision to the proto- Philippine arc in Miocene, as the results of this deformation, NE-SW direction wave folding occurs in the northeastern part and thrusts of various directions occur in the southwestern part.

2-1-1-2 The Southern Part

The Southern Part is basically composed of uplifted Cretaceous to Paleogene formations and an ophiolite suite which is overthrusted on the former formations.

The period of thrusting is inferred to be from the Late Eocene to the Middle Miocene time.

Associated with the ophiolite suites observed in the southern part are the Oligocene to Pliocene formations. Late miocene and Pliocene formation overlie in part the ultramafic units.

2-1-2 Stratigraphy (Ref. Figures 4, 5)

The stratigraphic sections agreed upon during the Workshop in Manila on June, 1988 are shown in Figures 4 and 5.

(Fig. 4 Stratigraphic Column of the Northern Part of the Area)

(Fig. 5 Stratigraphic Column of the Southern Part of the Area)

2-1-2-1 The Northern Part

The Northern Part is divided geologically into the northeastern zone and southwestern zone by the thrust which passes form the Kapoas Peninsula in the west side to the Calauag Bay in the east side.

2-1-2-1-1 The northeastern zone

The structure of this zone is controlled by two anticlines which show NE-SW direction and observe at Busuanga Island to Pancol. The lower formations, Bacuit Formation and Minilog Limestone (Permian to Triassic in age) are observed at the axial part of these anticlines while the upper formation, Busuanga Formation (Jurassic in age) is distributed along the limbs of the anticline.

Outcrops of the Guinlo Formation which has been dated as Cretaceous were encountered at the Busuanga Island and at the western side of the Calauag Bay in the northern part of Palawan Island. This formation, which unconformably overlies the Busuanga Formation, consists of massive quartzose sandstones with occurrences of mudstone and conglomerates.

The Bacuit Formation which is exposed at the vicinity of El Nido is dated as Middle Permian in age by the studies on fossils found in some chert samples. (Fontaine, 1981, Wolfart et al., 1984.)

2-1-2-1-2 The southwestern zone

The Caramay Schist and the Concepcion Phyllite forming the basement rocks in this zone are thrusted over the Panas Formation and Busuanga Formation at the western and northern sides respectively.

The Caramay Schist and the Concepcion Phyllite cover almost the entire area.

The metamorphic rocks have been considered to be Carboniferous to Permian in age by MGB (1981), but it was pointed out recently that these metamorphic rocks could probably be derived from some Cretaceous or Paleogene turbidite formations (R. A. Santos, 1988, oral.).

The Caramay Schist consists of muscovite schist, quartz mica schist and graphite schist and is also characterized by an almost micafree quartzite.

The Concepcion Phyllite consists of phyllitic mudstone, siltstone, sandstone and meta-sediment, and is also associated with conglomeratic mudstone.

The Panas Formation is distributed along a narrow area from the eastern part of the Ulugan Bay to the eastern portion of Pandanan Bay. The Concepcion Phyllite is thrusted over this formation.

This formation which is assumed to be of Eocene age is inferred to have been a submarine fan deposit. It is composed of tightly

folded, faulted and imbricated units of quartzo-feldspathic sandstone, mudstone and shale.

St. Paul's Limestone is observed at the east side of Mt. St. Paul Bay with a northeast trend consisting of massive dark gray limestone and contains abundant algae, coralline detritus and foraminifera fossils which were dated as Late Oligocene to Middle Miocene age (BMG, 1981; UNDP, 1985).

2-1-2-2 Southern Part

2-1-2-2-1 The basement complex

The basement of the Southern Part consists of the Sulu Sea Mine Formation, the Tagbros Formation and the Espina Basalt. The Sulu Sea Mine Formation consist of chert, mudstone and conglomerate and the Tagbros Formation is composed of green siltstone with wacke and conglomerate. Aside from being exposed as windowlike-inliers at a small spot north of Puerto Princesa, these basement rocks are distributed east of Quezon, around the southwestern portion of the mountain range of this Part and in the Balabac Island.

These basement units are dated as Cretaceous in age.

2-1-2-2-2 Tertiary Formation

The Panas Formation is a turbidite formation which is composed of shale, mudstone and alternating arkoase sandstone and is distributed at the west side of the Ulugan Bay, the periphery of the Pulot area and at the southwestern part of this area.

The Panas Formation is associated with and partially alternates with the Sumbiling Limestone which is thought to be a contemporaneous heteropic facies of the Panas Formation.

The Pandian Formation is basically made up of arkoarse sandstone associated with shale and siltstone, and considered to be Lower Oligocene in age. It is distributed at the west coast of the southwestern side of Quezon, overlying the Panas Formation unconformably.

The Ramsang Limestone composed of sandy and silty limestone is estimated to be Early Miocene age. It has a limited distribution at the eastern side of Quezon and at the eastern and northeastern portion of Rio Tuba.

The Isgod Formation is composed of alternating sandstone, mudstone and siltstone is associated with coralline limestone. It is distributed at the east and southern sides of Quezon and is dated to be to Middle Miocene in age.

The Alfonso XIII Formation consists basically of reefal limestone and overlies the Isgod Formation. This formation is distributed around the Aboabo area in the south and is found to be Late Miocene in age.

The Sayab Formation consisting of alternating sandstone and shale beds and is exposed at the southwestern part of Rio Tuba. It is to be Late Miocene in age. Similar to the Alfonso XIII Formation.

The Clarendon Formation consists of alternating sandstone to shale and is distributed at the southern part of Balabac Island and is found to be Pliocene in age.

The Iwahig Formation which is composed of conglomerate and limestone bodies is distributed from Puerto Princesa to Narra in the southeastern coast and at the vicinity of Wangle in the southernmost portion of the main Palawan Island. It is found to be Pleistocene in age as based on paleontological studies.

2-1-3 Geologic Structure

The Palawan area is divided into the Northern Part and the Southern Part, in which the Sabang thrust is considered as the tectonic boundary. The Northern Part is composed mainly of sedimentary and metamorphic rocks and includes continental block materials believed to have been deposited at the southern margin of the Asian continent (Taylor and Hayes, 1980, 1983). The Southern Part, on the other hand, has a basement composed essentially of an oceanic crust and lurbiditic sediments in which an opniolite suite was overthrusted (Sautos, 1988).

2-1-3-1 The Northern Part

The cherty sediments in the northeastern portion of the Northern Part are believed to have been deposited at the southern margin of Mainland Asia. The section of the mainland Asia containing these sediments drifted southward in which the movement is attributed to crustal thining and ocean crust formation. Collision of this continental fragment to Proto-Philippine Arc in Middle Miocene time (Holloway, et al. 1981), leading to its present configuration as observed today.

The collision resulted in the formation of NW-SE trending folds that observable in the northeastern portion of the main Palawan Island and in the Calamian Islands Group.

The Concepcion Phyllite which is derived from alternating sandstone and mudstone is mainly distributed throughout the southwestern portion of the Northern Part thrusted over the cherty sediments at the northeastern portion and the Panas Formation at the northwestern side.

2-1-3-2 The Southern Part

The suduction with the northwest direction to the assumed trench which was inferred to locate in the southwestern part of South China Sea had terminated by the late Eocene, the deposition of the Panas Formation was carried out in this last stage.

The Sulu sea, at the time, was also spreading in a NW-SE direction resulting into the formation of new oceanic crusts. These oceanic materials were thrusted over the Panas Turbidite and other Paleogene Formations. The thrusting event is inferred to have continued until Middle Miocene resulting in to the thrusting of the oceanic materials over the Oligocene Pandian Formation. The Mt. Beaufort ultramafic rocks which are extensively exposed at the central mountain range in the Southern Part and the Sabang Thrust at the east side of Ulugan Bay and adjacent thrust are thought to be directly related, in on way or another, to these thrust movements (Mitchel, et al., 1985).

The fault which cuts the Alfonso XIII Formation at the west of Quezon in a NW-SE direction and in a westward dip is the only one recognized as a post Miocene fault.

2-1-4 Igneous Activities

2-1-4-1 The Northern Part

Only three igneous bodies are known to occure in the Northern Part, namely, the Kapoas Intrusives, the Mangunao Volcanics and the Ultramafics of Paly Island.

The Kapoas Intrusives are observed as several stocks trending NNE the east from the east side of El Nido through the Kapoas Peninsula to the east side of the Ulugan bay in the vicinity of Stripe Peak. These stocks are dated Late Eocene to Early Oligocene by K-Ar method. (UNDP, 1984; MMAJ, 1987)

The Manguao Volcanics are observed as volcanic flows at the southern part of Manguao Lake in the northeastern main Palawan Island.

The Ultramafics are observed at Paly Island which is located offshore at the northeast of the Northern part. These ultramafics are believed to be thrusted over the north Palawan block and contain chromite dissemination.

2-1-4-2 The Southern Part

The igneous rocks in the Southern Part is composed of basalt extrusives, thrusted ultramafics and the associated gabbros on both rock units. Dikes of pyroxynite and gabbro are widespread throughout the abovementioned rock units.

The Espina Basalt which is believed to be part of the basement and is of Cretaceous age is exposed as a windowlike-inlier in an area north of Puerto Princesa and in many localities with in Central and South Palawan areas.

The Mt. Beaufort Ultramafics are mainly made up of harzburgite with irregular patches and lenses of dunites. Chrome spinel/chromites are known to exist and to occur as disseminations in these rocks. These ultramafics are presumed to be of Eocene age.

The Stavely Range Gabbro along with the Mt. Beaufort Ultramafics constitute the Palawan Ophiolite which is thrusted over the Early Oligocene pandian Formation and the Eocene Panas Formation. The thrusting is inferred to have occurred throughout the Eocene to Middle Miocene, although the inception of this activity is thought to have started during the Paleocene.

2-2 Mineralization
(Major Mineral showings are shown on Table-1, Table-2)

In general, the mineralizations in the Palawan area is prior intense in the Southern Part.

2-2-1 The Northern Part

The field survey conducted revealed four kinds of mineralization as follows: (*1 the number listed for the mineral showings correspond to the number Table-1 and 2)

(A) Strata-bound manganese mineralization in cherty rocks at the eastern part of Busuanga Island
(64. Lanka; 65. Dapdapan)*1

(B) Vein type manganese mineralization in sedimentary rocks at the northern part of Culion Island
(4. Kabol-Kabol)

(C) Chromite dissemination in ultramafics at Paly Island
(66. Paly Is.)

(D) Stibnite mineralization associated with quartz vein in mica shcist at the northwestern part of Tinitian

2-2-2 The Southern Part

The field survey conducted revealed four kinds of mineralization as follows.

(A) Chromite lenses in ultramafics
(67. Richman; 68. Boyo; 62. Berong; 77. Trident, etc.)

(B) Nickel-laterite mineralization which are weathering products of the ultramafics
(26. Atlas mine; 71. Ibat-ong; 73. Bethlehem; 76. Santa Monica; 39. Pulute Rnge; 54. Rio Tuba; etc.).

(C) Cyprus type massive sulfide copper mineralization
(78. 79. 80. Barong Barong A, B, C; 81. Males, etc)

(D) Sulfide bearing quartz vein type mineralization
(1. Pulot, etc.)

The operating mines in the Southern Part are the Atlas Mine (ATLAS Corp.) and the Rio Tuba Mine (Rio Tuba Nickel Corp.). The details of these mines are as follows.

(A) Atlas Mine (Also called Berong Point Mine)

The ores of this mine consist of chromite gravel in laterite. This mine is located 5 km southwest of Long Point in the northwestern coast.

This mine started operating at the end of 1985 and has shipped concentrates at a rate of 1,147 ton per month. The country rock is serpentinite, the alteration product of ultramafic rocks.

Pit sample grades of this mine are as follows:

Sample No.	SiO_2	Cr_2O_3	Fe_2O_3	MgO	Al_2O_3	Total
Ca007	0.4%	53.1%	10.3%	13.7%	17.4%	94.9%
Ca008	0.4%	51.1%	11.0%	13.1%	17.0%	92.5%
Ca009A	0.6%	47.1%	11.7%	12.6%	19.2%	91.2%
Ca009B	0.2%	54.3%	9.5%	14.5%	16.5%	95.0%

(JICA · MMAJ, 1987)

(B) Rio Tuba Mine

The deposit of this mine is a nickel-laterite type, a weathering product of ultramafic rocks. Rio Tuba Nickel Corporation has been operating since 1977 and has been producing 500,000 tons of concentrates per year (average grade: Ni: 3.3%; Co: 0.04% and moisture: 30%). It has a proven reserve of 9,600,000 tons with an average grade of 2.3% Ni and a stripping ratio of 1:1. At present, 550 personnel are employed in the mine. At the surface is a 5 m thick reddish black to reddish brown lateritic soil. Beneath of this soil is a 2 - 5 m thick mineralized zone.

GEOLOGIC TIME					BMG	JICA AND MMAJ	RP–JAPAN WORKSHOP (1988)			
DATE	ERA	PERIOD	EPOCH	AGE	1981*1	1987, 1988	FORMATION	LITHOLOGY	IGNEOUS ACTIVITY	REMARKS
0.01	CENOZOIC	QUATERNARY	HOLOCENE		Quaternary Alluvium Raised Beaches	Alluvium Coral reef	Alluvium			
			PLEISTOCENE	L E	Manguao Volcanics	Manguao Volcanics (Ma)	Manguao Volcanics	Aphanitic highly vesicular basalt flow	Manguao Volcanics (mainly basalt flow)	
1.8			PLIOCENE	E	?					
5.0				E						
		TERTIARY	MIOCINE	M	Piedras Point Andesite	Piedras Point Andesite				
22.5				E	St. Paul's Ls.	St. Paul's Ls. ?	St. Paul's Ls.	Massive reefal limestone, rich in algae, corals and Foraminifera fossils		• ST. Paul's limestone is dated Late Oligocene to Middle Miocene by K-Ar Method (UNDP, 1985)
			OLIGOCENE	L	Siltstone, sand stone, shale, pillow lava	Babuyan River Turbidites (Bt)				
38.0				E	?	?			Kapas Intrusives	• Kapoas Intrusives is dated Late Eocene to Early Oligocene by K-Ar method, by UNDP and RP-JAPAN Project. (UNDP, 1984. JICA and MMAJ. 1987.)
			EOCENE	L	Pabellion Ls.	Pabellion Ls. (Pa)	Pabellion Limestone / Panas F.	Massive crystalline fossiliferous limestone / Quartzose sand stone, interbedded with shale and mudstone U.R	Palawan Ultramafics	• Isolated outcrop of Palawan Ultramafics is distributed.
				E						
55.0			PALEOCENE	L						
65.0				E						
	MESOZOIC	CRETACEOUS		L	Serpentine, gabbroo	Serpentine, gabbroo	Boayan Turbidites / Guinlo F.	Massive quartz-felôspathic sandstone, weakily metamorphosed / Massive quartz rich sandstone, interbedded with mudstone and conglomerate.		
				E	?					
141		JURASSIC		L	Kapoas Granite	Kapoas Granite	Imorigue Ls.			
				H	Guinlo F.	Guinlo F. (Gn)	Busuanga Chert	Red and gren chert / Massive or bedded reefal and micritic limestone		
				E	Limestone, shale and sandstone					
195		TRIASSIC		L			Liminangcong Chert / Coron Ls.	Similar to Busuanga Chart, but redioraliar asseblage show different ages / Crystalline reefal and massive limestone		• Jurassic chert units are assigned to Busuanga Chert
				M	Liminangcong F.	Liminangcong F. (Li)				• Late Permian to Late Triassic chert units are assigned to Liminangcong chert.
				E	?		Minilog Ls.	Massive limestone partly crystalline and colitic		
250	PALEOZOIC	PERMIAN		L	Minilog F.	Minilog F. (Mi)				
				M	Bacuit F. ?	Bacuit F. (Ba)	Bacuit F ?	Alternation of sandstone and shale with chert, Cgl. and Ls.		
				E		Tumarbong Semischist				
280		CARBONFEROUS			Barton Metamorphics	Danleg Sandstone / Cocepcion Conglomerate / Caramay Schist	Concepcion Phyllite ? / Caramay Schist ?	Phyllitic mudstone, siltstone, shale and fine sandstone / Muscovite schist		

*1 BMG, Geology and Mineral Reources of the Philipines, 1981 Vol. I p. 26 (Table II).

*2 U.R.: Plawan Ultramafic Rocks

Fig. 4 Stratigraphic Column of the Northern Part of the Area

GEOLOGIC TIME					BMG	JICA AND MMAJ	RP JAPAN WORKSHOP (1988)			
DATE	ERA	PERIOD	EPOCH	AGE	1981*1	1987, 1988	FORMATION	LITHOLOGY	IGNEOUS ACTIVITY	REMARKS
0.01	CENOZOIC	QUATERNARY	HOLOCENE		Quaternary Alluvium	Recent sediments (Qt)	Alluvium	Coral reef, detrital depoits, sand, silt, clay		
1.8			PLEISTOCENE	L E	Tagburos Opalite					
		TERTIARY	PLIOCENE	L E	Iwahig F.	N2 F. (N2)	Iwahig F. / Clarendon F.	Pusok Cgl. Panoyan Ls. / Interbedded sandstone and shale.		
5.0			MIOCINE	L	Alfonso XIII F.	N1 Ls. (N1Ls)	Alfonso / Sayab F.	Coral reef ls. and marl / Quartzose ss. and shale..		
				M	Isgod F.		Isgod Formation	Interbedded shale and sandstone with coral ls.		
				E	Ransang limestone	N1 F. (N1)	Ramsang Limestone	Massive sandy to silty limestone.		
22.5						N1 Pyroclastics				
			OLIGOCENE	L E	Pandian F.		Pandian F.	Massive arkose ss. with mudstone, shale, siltstone		
38.0			EOCENE	L E	Panas F. / Sumbiling Limestone		Sumbiling Limestone / Panas F.	Massive crystalline ls. interbedded with Panas F. / Quartzose ss. interbedded shale and mudstone		• Stavely Rangely Gabbro is dated Late Eocene by K-Ar method (Remmlmair, 1985)
55.0			PALEOCENE	L E	?				Stavely Range Gabbro Mt. Beaufort Ultramafics	
65.0	MESOZOIC	CRETACEOUS		L	Quartz diorite Stavely Range Gabbro Mt. Beaufort Ultramafices	K F. (K) / Gb	Tabros Siltstone / Sulu Sea Mine F. / Espina Basalt San Visente Gabbro	Green siltstone with wacke and conglomerate. Chert, mudstone and conglomerate.	Espina Basalt San Vicente Gabbro	• Espina Basalt is dated Late Cretaceous by the study of radioralian assemblage of interbedded chert
				E	?					
141		JURASSIC		L M E	Irahauan Metamorphics	Ultramafics (Uc)				
195		TRIASSIC		L M E	? Schist ?	Meta-morphics (Gd) (Gd)				
250		PERMIAN		L M E						
280	PALEOZOIC	CARBONIFEROUS			Altered arkose					

*1 BMG, Geology and Mineral Reources of the Philipines, 1981 Vol. I. p. 28 (Table II-5).

Fig. 5 Stratigraphic Column of the Southern Part of the Area

Table-1 Major Mineral Showings in the Northern Part

Mineral showings investigated by RP-Japan Project (1986-1987) in northern Palawan Area

*1 MINERAL SHOWING NAME	LOCATION	COMMODITY AND MINERALIZATION	AGE	TECTONIC PROVINCE	DESCRIPTION	
					OCCURENCE	CHEMICAL ASSAY OF SAMPLE
4 Kabol-Kabol	119°54' E 11°52' N	Mn Vein	Post Paleozoic	Continental block	Manganese dioxide and rhodochrosite accompanied calcite vein in chert.	Calcite vein sample (w ; 10 cm); MnO 19.90%, P_2O_5 0.85%, SiO_2 53.03%.
64 Lanka	120°13' E 12°03' N	Mn Sedimentary	Post Paleozoic	Oceanic crust	Lenticular maganese body in chert, cryptomelane and pyrolucite observed.	Brecciated sample; MnO 13.2%, P_2O_5 0.27%, SiO_2 78.07% Massive sample; MnO 42.96%, P_2O_5 0.44%, SiO_2 33.03%.
65 Dapdapan	120°19' E 12°01' N	Mn Sedimentary	Post Paleozoic	Oceanic crust	Lenticular manganese body in chert, psilomelane and pyrolucite observed.	Banded sample; MnO 22.06%, P_2O_5 0.28%, SiO_2 63.60%.
66 Paly Is.	119°42' E 10°43' N	Cr Dissemination	Cretaceous	Oceanic crust *2	Chromite dissemination in ultramafic rock.	

*1 These numbers are corresponded to the numbers in Attached Plate 8-1.

*2 Chromite formed in oceanic crust which was thrusted over the North Palawan Block.

Table-2 Major Mineral Showings in the Southern Part

Mineral showings investigated by RP-Japan Project (1986-1987) in southern Palawan Area

*1 MINERAL SHOWING NAME	LOCATION	COMMODITY AND MINERALIZATION	AGE	TECTONIC PROVINCE	DESCRIPTION	
					OCCURENCE	CHEMICAL ASSAY OF SAMPLE
26 Atlas mine	118°25' E 9°38' N	Cr Orthomagmatic	Post-Cretaceous	Oceanic crust	Operating (refer text)	
39 Pulute Range	117°57' E 9°04' N	Ni Laterite	Post-Cretaceous	Oceanic crust	Laterite area is 2 km^2 (depth, over 3.5 m) garnierite, veinlet in dunite.	Lateritic soil sample (w ; 3.2 m); Fe_2O_3 19.61%, Al_2O_3 3.11%, MgO 0.66%, Ni 1.24%, Cr 2.91%
54 Rio Tuba	117°25' E 8°34' N	Ni Laterite	Post-Cretaceous	Oceanic crust	Operating (refer text)	
56 Balabac	117°04' E 7°59' N	Cu Cyprus type massive sulfide	Eocene	Oceanic crust	Mineralization, consists of Pyrite, chalcopyrite, bornite and sphalerite.	Massive sulfide sample; Cu 3.07%, Pb 0.01% Zn 0.06%, Ag 11.8 g/t, Au 0.69 g/t
62 Berong	118°14' E 9°25' N	Cr Orthomagmatic	Cretaceous	Oceanic crust	Leticular chromite bodies in dunite.	Chromite high condenced sample; FeO 11.81%, Al_2O_3 19.57%, MgO 18.85%, NiO 0.23%, Cr_2O_3 42.6%.
67 Richman	118°28' E 9°37' N	Cr Orthomagmatic	Cretaceous	Oceanic crust	Lenticular chromite bodies in peridotite.	Chromite condenced sample; Cr_2O_3 28.1 - 48.8%, Total Fe 7.3 - 8.6%.
68 Boyo	118°29' E 9°42' N	Cr Orthomagmatic	Cretaceous	Oceanic crust	Lenticular chromite bodies in peridotite.	Chromite condenced sample; Cr_2O_3 34.0 - 50.5%, Total Fe 9.1 - 9.8%.
69 Benguet	118°37' E 9°50' N	Cr Orthomagmatic	Cretaceous	Oceanic crust	Lenticular chromite bodies in peridotite.	Chromite condenced sample; Cr_2O_3 23.9 - 59.0%, Total Fe 7.6 - 9.2%.
70 Romarao	118°15' E 9°29' N	Cr Orthomagmatic	Cretaceous	Oceanic crust	Dotted chromite in lateritic soil.	Chromite condenced soil sample; Cr_2O_3 41.08, Fe_2O_3 11.24%.
71 Ibatong	118°22' E 9°25' N	Ni Residual	Post-Cretaceous	Oceanic crust	Nickeliferous laterite. (thickness ; 2 m)	Laterite sample; Fe_2O_3 66.51%, Al_2O_3 7.19%, NiO 0.80%, MgO 1.02%.
72 Malasgao	118°24' E 9°24' N	Ni Residual	Post-Cretaceous	Oceanic crust	Nickeliferous laterite. (area ; 2.5 km^2, thickness ; <2 m)	Laterite sample; Fe_2O_3 56.73%, Al_2O_3 7.19%, NiO 1.09%, MgO 2.33%.
73 Bethlehem	118°19' E 9°18' N	Ni Residual	Post-Cretaceous	Oceanic crust	Nickeliferous laterite. (area ; 7 km^2, thickness ; <5 m)	Laterite sample; Fe_2O_3 54.62%, Al_2O_3 6.89%, NiO 1.66%, MgO 3.93%.
74 Bethlehem west	118°16' E 9°18' N	Ni Residual	Post-Cretaceous	Oceanic crust	Nickeliferous laterite. (area ; 3 km^2, thickness ; <5 m)	Laterite sample; Fe_2O_3 54.62%, Al_2O_3 6.89%, NiO 1.66%, MgO 3.72%.
75 Olympic	118°16' E 9°13' N	Ni & Cr Residual and orthomagmatic	Post-Cretaceous	Oceanic crust	Chromite lenticular bodies in serpentinized peridotite.	Chromite lens sample (30 cm); Cr_2O_3 47.94%, NiO 0.11%.
76 Santa Monica	118°14' E 9°13' N	Ni Residual	Post-Cretaceous	Oceanic crust	Nickeliferous laterite.	Laterite sample; Fe_2O_3 64.54%, Al_2O_3 5.15%, NiO 1.64%, MgO 1.53%.
77 Trident	118°21' E 9°19' N	Cr Orthomagmatic	Cretaceous	Oceanic crust	Chromite lens in dunite. (pit wall sample width ; 2 m)	Pit wall sample; Cr_2O_3 44.81%, FeO 13.60%, Al_2O_3 4.8%, MgO 0.18%.
78, 79, 80 Barong-Barong A. B. C.	117°49' E 8°56' N	Cu Cyprus type massive sulfide.	Eocene	Oceanic crust	Lenticular massive sulfide in basalt. Pyrite chalcopyrite and sphalerite are observed.	Massive to clastic sulfide sample; Cu 6.52 - 0.20%, Zn 0.23 - 0.01%, Ag 52 - 7g/t, Au 0.21 - <0.07g/t.
81 Males	117°43' E 8°46' N	Cu Cyprus type massive sulfide.	Eocene	Oceanic crust	Lenticular massive sulfide in basalt. Ore minerals are pyrite chalcopyite and sphalerite.	Massive sulfide sample; Cu 0.52%, Pb 0.02%, Zn 0.19%, Ag 13.3g/t.
82 Pulot	117°56' E 8°59' N	Cu vein	Eocene	Oceanic crust	Quartz vein in altered basalt. Vein system shows N50°- 60°E strike and 40°- 60°SE dip.	Vein (w ; 15 cm) sample; Cu 1.42%, Zn 0.01%, Ag 6.5g/t.

*1 These numbers are corresponded to the numbers in Attached Plate 8-2.

3. Geochemical SampleAnalyses and DataProcessing

3-1 Analytical Methods

A total of 8,426* stream sediment samples (* the numbers in cludes 2,250 samples collected by L'NDP., 1985) (less than 0.175 mm) were collected in the Palawan area.
sections in charge of laboratory research. Microchemical analyses were carried out by atomic absorption spectroscopy (AAS).

Analyzed elements are as follows.

For the Northern Part: Cu, Pb, Zn, Ag, As, Mn, Ni, Co, Mo, Hg, Cr, Sb, Sn and W

For the Southern Part: Cu, Pb, Zn, Ag, As, Mn, Ni, Co, Hg and Cr.

Analytical flow charts are shown in Appendixes 2-1 to 2-4.

3-1-1 Precision and Accuracy Checks

Detection limit values of AAS analyses in PETROLAB are as follows.

Table-3 Detection Limit VCalues of AAS Analyses (ppm)

Element	Cu	Pb	Zn	Ag	As	Mn	Ni	Co	Mo	Hg	Cr	Sb	Sn	W
Detection limit value	2	10	2	1	0.5	50	3	3	2	0.04	100	0.05	1	3

Precision checks of chemical analyses results were carried out. The variance of analyzed values at 95% confidence level is calculated by the method of Thompson and Howarth (1973) with the result of the batch test by PETROLAB.

The checked result is given as follows:

A) Process of the batch test

A sample is chosen from each analyzed batch (about 20 samples) and is analyzed with another batch, after which the variance is calculated by the statistical procedure with the former and latter values.

B) Results of the precision check

Table-4 Dispersion of Batch Test Results

Element	Variance	Remark
Cu	±15%	The variance of Ag and Mo can not be determined because many samples contained these elements below detection limit.
Pb	±20%	
Zn	±20%	
As	±25%	
Mn	±10%	
Ni	±20%	
Co	±20%	
Hg	±25%	
Cr	±30%	
Sb	±25%	

3-2 Data Processing

The survey area where 8,426 stream sediment samples were collected is divided into 3,390 cells (2km × 2km) based on the datum point (117° 00' east longitude, 8° 20' north latitude). The geometric average of the result of analyses of each cell is calculated.

The four kinds of statistical analyses method were conducted on these cell average values. These methods are as follows:

(A) Univariate analyses of the geometrical average values of the results of chemical analyses of each cell. (hereafter called cell average value)

(B) Univariate analyses of the moving average value which the average value of nine cells is estimated to be the value of the central cell.

(C) Univariate analyses of the high-pass filter value which is the positive difference when the moving average value is deducted from the cell average value.

(D) Multivariate analyses (Factor Analyses) for cell average value.

IBM3084Q computer and statistical analyses package BMD 08M (UCLA developed) are utilized on statistical procedure.

All geochemical average values input the computer with logarithmic value and the results were transferred to normal value.

For the purpose of the statistical procedure. The 50% values of the detection limit are given the cells which have the geometric average value below the detection limit.

As for Ag, the all cells showed the cell average values below the detection limit value were except two cells, and the all cell average values of Mo showed below the detection limit value, thus Ag and Mo were omitted from these statistical analysis.

3-2-1 Univarate Analyses

3-2-1-1 Cell Average Values of the Northern Part

The Northern Part where 4,219 stream samples have been taken is divided into 1,667 cells (2 km × 2 km).

The geometric average of the results of analyses of each cell was calculated. The average number of samples is 2.56 per each cell. For blank cells with no sampling point, gap filling is done as follows.

Geometrical average value of the eight cells around the blank cells is applied as the values of the blank cell. When the effective values are less than four cells, gap filling is not done. This gap filling procedure was done twice.

Table-5 Basic Statistical Values forth Cell Average Values (Northern Part)

	Cu (ppm)	Pb (ppm)	Zn (ppm)	Ag (ppm)	As (ppm)	Mn (ppm)	Ni (ppm)	Co (ppm)	Mo (ppm)	Hg (ppb)	Cr (ppm)	Sb (ppb)	Sn (ppm)	W (ppm)
$\overline{X}$	8.03	5.86	23.11	0.50	3.53	170.51	7.84	3.90	1.00	27.56	72.43	116.97	0.52	1.53
$\overline{X}+1.0\ \sigma$	16.51	7.84	49.13	0.51	8.25	427.90	19.46	8.30	1.00	48.67	154.86	291.90	0.65	1.78
$\overline{X}+1.5\ \sigma$	23.67	9.07	71.63	0.51	12.62	677.86	30.67	12.12	1.00	64.68	228.23	461.11	0.73	1.92
$\overline{X}+2.0\ \sigma$	33.94	10.49	104.44	0.52	19.28	1,073.83	48.32	17.68	1.00	85.95	331.12	728.41	0.82	2.07
Minimum	1.00	5.00	1.00	0.50	0.25	25.00	1.50	1.50	1.00	20.00	50.99	25.00	0.50	1.50
Maximum	94.00	22.00	182.00	1.00	94.00	6,00.00	4,000.00	360.00	1.00	20,000.00	108,000.00	6,560.00	12.00	33.47
Number of cells	1,667	1,667	1,667	1,667	1,667	1,664	1,664	1,664	949	1,667	1,665	1,667	1,312	1,312
R.B.D.	4.6 %	91.6 %	1.0 %	99.9 %	1.7 %	10.3 %	13.2 %	39.5 %	100 %	80.1 %	80.7 %	19.7 %	97.7 %	99.2 %

$\overline{X}$: Mean value σ : Standard deviation R.B.D. : Ratio of below detection limit value

Table-6 Basic Statistical Values of the Original Analyses (Northern Part)

	Cu (ppm)	Pb (ppm)	Zn (ppm)	Ag (ppm)	As (ppm)	Mn (ppm)	Ni (ppm)	Co (ppm)	Mo (ppm)	Hg (ppb)	Cr (ppm)	Sb (ppb)	Sn (ppm)	W (ppm)
$\overline{X}$	8.09	6.08	25.48	0.50	3.64	175.68	8.71	4.04	1.00	28.95	75.42	109.74	0.52	1.52
$\overline{X}+1.0\ \sigma$	17.39	8.98	56.42	0.51	10.01	470.56	27.43	9.99	1.00	57.21	232.88	311.49	0.68	1.83
$\overline{X}+1.5\ \sigma$	25.51	10.92	83.97	0.51	16.60	770.12	48.66	15.71	1.00	80.43	409.21	524.77	0.79	2.01
$\overline{X}+2.0\ \sigma$	37.41	13.28	124.97	0.52	27.55	1,260.37	86.34	24.71	1.00	113.08	719.08	884.09	0.90	2.20
Minimum	1.00	5.00	1.00	0.50	0.25	25.00	1.50	1.50	1.00	20.00	50.00	25.00	0.50	1.50
Maximum	173.00	44.00	410.00	2.00	210.00	15,000.00	4,480.00	430.00	1.00	20,000.00	108,000.00	9,999.00	25.00	250.00
Number of cells	4,219	4,219	4,219	4,219	4,219	4,208	4,207	4,160	1,781	4,219	4,163	4,219	2,475	2,475

$\overline{X}$: Mean value σ : Standard deviation

3-2-1-1-1 Basic statistical values

The basic statistical values of the cell average analyses for each element are shown on Table-5, and the basic statistical values of the original analytical results are shown in Table-6 for reference purposes.

3-2-1-1-2 Histograms and cumulative frequency curves

Histograms and cumulative frequency curves are shown in the attached plates at the end of this volume (Appendix 1-1 and 1-2).

The ranges of anomalous values as determined from the study of these data are as follows:

Cu: Inflection point of the curve is at the point 80% which corresponds to $\overline{X}+1.0\ \sigma$ value (15 ppm). This value was used as the threshold value.

Pb: About 91.6% of the cells contained amount below detection limit values. The limit of the anomalous values is therefore not clear.

Zn: Inflection point of the curve is at the point 93% cumulative frequency which corresponds to $\overline{X}+1.0\ \sigma$ value and $\overline{X}+1.5\ \sigma$ value (60 ppm). This value was used as the threshold value.

As: The curve shows inflection point at 96% which corresponds to $\overline{X}+1.5\ \sigma$ value and $\overline{X}+2.0\ \sigma$ value (7 ppm). This value was used as the threshold value.

Mn: Inflection point of the curve is at 98% which corresponds to $\overline{X}+2.0\ \sigma$ value (1,030 ppm). This value was used as the threshold value.

Ni: The curve shows inflection point at 97% which corresponds to the value $\overline{X}+2.5\ \sigma$ value (60 ppm). This value was used as the threshold value.

Co: The curve shows inflection point at 90% which corresponds to $\overline{X}+1.0\ \sigma$ value (10 ppm). This value was used as the threshold value.

Mo: All of the cells show below detection limit values, thus the Mo values were omitted from the statistical analysis.

Hg: About 80% of the cells contained amount below detection limit values, thus the range of the anomalous values was unclear.

Cr: About 80% of the cells contained amount below detection limit values, so the cumulative frequency curve is out of the logarithmic normal dispersion, but the inflection point is still observed at 97% which corresponds to over $\overline{X}+2.0\ \sigma$ value (400 ppm). This value ws used as the threshold value.

Sb: The curve shows inflection point at 99% which corresponds to the value a little over $\overline{X}+2.0\ \sigma$ value (850 ppb). This value was used as the threshold value.

Sn: About 98% of the cells contained amount below detection limit values, thus the range of the anomalous values was unclear.

W: About 99% of the cells contained amount below detection limit values, thus the range of the anomalous values was unclear.

3-2-1-1-3 Correlation coefficients between each element

Correlation coefficients among the elements are shown on Table-7 and Table-8.

Table-7 Correlation Coefficients (between Elements) in Cell Average Values (Northern Part)

	Cu	Pb	Zn	Ag	As	Mn	Ni	Co	Mo	Hg	Cr	Sb	Sn	W
Cu	1.000													
Pb	0.211	1.000												
Zn	0.720	0.315	1.000											
Ag	0.011	- 0.014	0.011	1.000										
As	0.444	0.267	0.415	0.024	1.000									
Mn	0.749	0.231	0.737	0.022	0.420	1.000								
Ni	0.597	0.168	0.745	0.012	0.265	0.731	1.000							
Co	0.710	0.232	0.681	- 0.009	0.322	0.803	0.812	1.000						
Mo	—	—	—	—	—	—	—	—	1.000					
Hg	0.342	0.133	0.262	- 0.014	0.094	0.348	0.398	0.375	—	1.000				
Cr	0.259	- 0.145	0.170	- 0.012	- 0.043	0.245	0.556	0.459	—	0.238	1.000			
Sb	0.254	0.025	0.082	0.029	0.492	0.025	0.118	0.180	—	0.159	0.075	1.000		
Sn	- 0.068	- 0.037	- 0.001	- 0.005	- 0.055	- 0.001	- 0.015	- 0.031	—	- 0.044	- 0.029	- 0.052	1.000	
W	- 0.013	0.929	0.025	- 0.004	0.045	- 0.030	- 0.023	- 0.020	—	- 0.051	- 0.040	- 0.032	0.249	1.000

Table-8 Correlation Coefficients (between Elements) in Original Analyses (Northern Part)

	Cu	Pb	Zn	Ag	As	Mn	Ni	Co	Mo	Hg	Cr	Sb	Sn	W
Cu	1.000													
Pb	0.280	1.000												
Zn	0.733	0.313	1.000											
Ag	0.004	- 0.008	0.003	1.000										
As	0.364	0.223	0.337	0.025	1.000									
Mn	0.701	0.250	0.684	0.017	0.350	1.000								
Ni	0.604	0.135	0.638	0.004	0.141	0.631	1.000							
Co	0.632	0.242	0.605	- 0.017	0.188	0.719	0.777	1.000						
Mo	—	—	—	—	—	—	—	—	1.000					
Hg	0.255	0.176	0.250	- 0.003	0.067	0.282	0.325	0.327	—	1.000				
Cr	0.178	- 0.121	0.113	- 0.006	- 0.128	0.192	0.657	0.490	—	0.202	1.000			
Sb	0.221	0.093	0.079	0.016	0.479	0.196	0.022	0.093	—	0.124	- 0.077	1.000		
Sn	- 0.030	- 0.036	- 0.019	- 0.003	- 0.012	- 0.001	- 0.020	- 0.030	—	- 0.027	- 0.020	- 0.013	1.000	
W	0.009	0.007	0.015	- 0.002	0.047	- 0.028	- 0.012	- 0.014	—	- 0.027	- 0.025	- 0.007	0.085	1.000

In the cell average values, positive correlations are observed among the following elements.

Cu-Zn, Mn, Ni, Co

Zn-Mn, Ni, Co

Mn-Ni, Co

Ni-Co, Cr

3-2-1-1-4 Areal distribution of the cell average values (Attached plate 2-1-1 No.1 - No. 12)

The cell average values of each element are classified into 11 ranks and plotted on a 1:1,000,000 scale map with corresponding rank colors.

Classified ranges are as follows.

Code	Cumulative frequency range
A	99% ≦ Z
B	95% ≦ Z < 99%
C	90% ≦ Z < 95%
D	75% ≦ Z < 90%
E	60% ≦ Z < 75%
F	50% ≦ Z < 60%
G	40% ≦ Z < 50%
H	30% ≦ Z < 40%
I	20% ≦ Z < 30%
J	Detection limit < Z < 20%
K	Detection limit < Z

The areal distribution of the anomalous cell average values of the elements are as follows:

Eastern part of Busuanga Island.
(Anomalous elements; Cu, Zn, As, Mn, Ni, Co, Hg, Cr and Sb)

Southern part of Busuanga Island.
(Anomalous elements; Cu, Mn and Cr)

Eastern part of Coron Island.
(Anomalous elements; Cu, Zn, As and Hg)

Eastern part of El Nido to Mt. Kapoas.
(Anomalous elements; Cu, Zn, As, Mn, Ni, Co and Hg)

Southeastern part of Mt. Kapoas.
(Anomalous element; Sn)

Paly Island.
(Anomalous elements; Ni, Co and Cr)

Northwestern part of Tinitian.
(Anomalous elements; As and Sb)

East side of Ulugan Bay
(Anomalous elements; Mn, Ni, Co, Hg and Cr)

The following five zones can be understood by their respective geological settings, igneous activities and mineralizations.

(a) Eastern and south-central part of Busuanga Island: The Cretaceous Busuanga Chert is distributed in this zone and strata-bound type manganese showings are know. Except for manganese, the overlapping of the various elements is assumed to reflect the absorption capacity of pelitic materials in the cherty sediments.

(b) Eastern part of El Nido to Mt. Kapoas: Kapoas Diorite stocks intruded in this zone in a NNE to SSW direction. The overlapping anomalous values of the various elements is assumed to have been caused by hydrothermal alteration associated with the intrusion of the diorite.

(c) Paly Island: This island is composed of ultramafic rocks with chromite dissemination. The overlapping of the elements with anomalous values is principally due to this country rock.

(d) Northwestern part of Tinitian: Antimony mineral showings are known in this zone. The As and Sb anomalous value are ready explained by this mineral showing.

(e) East side of Ulugan Bay: The Sabang Fault which divides the Northern and the Southern Part passes through the west side of this zone, and is associated with the ultramafic rocks. Ni, Co and Cr anomalous values can be explained by the presence of the ultramafics rocks.

3-2-1-2 Call average value of the Southern Part

The Southern Part where 4,207 stream samples have been collected is divided into 1,623 cells (2 km × 2 km).

The geometric average of the results of analyses of each cell is calculated. The average number of samples is 2.59 per each cell. The gap filling procedure performed is similar to that of the Northern Part.

3-2-1-2-1 Basic statistical values

The basic statistical values of the cell average analyses for each element are shown on Table-9, and the basic statistical values of the original analytical results are shown in Table-10 for reference purposes.

Table-9 Basic statistical values for the cell Average values (Southern Part)

	Cu (ppm)	Pb (ppm)	Zn (ppm)	Ag (ppm)	As (ppm)	Mn (ppm)	Ni (ppm)	40.68Co	Hg (ppb)	Cr (ppm)
$\bar{X}$	21.16	6.03	44.50	0.50	0.95	640.54	223.90	31.98	40.68	3,134.48
$\bar{X}+1.0\ \sigma$	43.85	8.61	71.12	0.50	2.63	1,266.38	1,233.92	87.60	124.46	25,825.93
$\bar{X}+1.5\ \sigma$	63.13	10.29	89.90	0.50	4.37	1,780.58	2,896.67	145.00	217.67	74,131.19
$\bar{X}+2.0\ \sigma$	90.89	12.29	113.66	0.50	7.28	2,503.61	6,800.05	240.01	380.71	212,787.44
Minimum	1.00	5.00	3.00	0.50	0.25	25.00	1.50	1.50	20.00	50.00
Maximum	198.00	38.00	190.79	0.50	23.00	4,984.00	60,697.00	982.85	27,450.00	188,790.00
Number of Cells	1,623	1,545	1,623	1,623	1,623	1,623	1,623	1,545	1,623	1,545
R.B.D.	0.6%	88.0%	0%	100%	33.1%	0.5%	0.6%	1.9%	65.9%	8.9%

$\bar{X}$: Mean value σ : Standard deviation R.B.D. : Ratio of below detection limit value

Table-10 Basic Statistical Values of the Original Analyses (Southern Part)

	Cu (ppm)	Pb (ppm)	Zn (ppm)	Ag (ppm)	As (ppm)	Mn (ppm)	Ni (ppm)	Co (ppm)	Hg (ppb)	Cr (ppm)
$\bar{X}$	22.22	6.23	46.65	0.50	0.98	681.36	224.13	31.54	42.74	2,780.75
$\bar{X}+1.0\ \sigma$	49.12	9.82	79.71	0.50	3.06	1,508.31	1,423.94	94.31	162.11	27,946.21
$\bar{X}+1.5\ \sigma$	73.04	12.33	104.19	0.50	5.39	2,244.12	3,589.10	153.08	315.72	88,603.32
$\bar{X}+2.0\ \sigma$	106.50	15.49	136.19	0.50	9.50	3,338.89	9,046.42	282.00	614.88	280,896.29
Minimum	1.00	5.00	1.00	0.50	0.25	25.00	1.50	1.50	20.00	50.00
Maximum	800.00	81.00	270.00	0.50	45.00	6,800.00	53,000.00	1,290.00	510,000.00	300,000.00
Number of sample	4,207	3,903	4,207	4,207	4,207	4,207	4,207	3,902	4,207	3,903

$\bar{X}$: Mean value σ : Standard deviation

3-2-1-2-2 Histograms and cumulative frequency curves

Histograms and cumulative frequency curves are shown in the attached plates at the end of this volume (Appendix 1-1 and 1-2).

The ranges of anomalous values as determined from the study of these data are as follows:

Cu: Inflection point of the curve was at the point 76% which corresponds to $\bar{X}+1.0\ \sigma$ value (36 ppm). This value was used as the threshold value.

Pb: About 88% of the cells contained amount below detection limit values. The limit of anomalous values was therefore not clear.

Zn: Inflection point of curve was observed at the point 80% which corresponds to $\bar{X}+1.0\ \sigma$ value (63 ppm). This value was used as the threshold value.

As: The curve shows inflection point at 88% which corresponds to $\bar{X}+1.0\ \sigma$ value (3 ppm). This value was used as the threshold value.

Mn: Inflection point of the curve was observed at 97% cumulative frequency which corresponds to values between $\bar{X}+1.5\ \sigma$ value and $\bar{X}+2.0\ \sigma$ value (2,000 ppm). This value was used as the threshold value.

Ni: The curve showed inflection point at 87% which corresponds to values between $\bar{X}+1.0\ \sigma$ value and $\bar{X}+1.5\ \sigma$ value (1,900 ppm). This value was used as the threshold value.

Co: The curve showed inflection point at 90% which corresponds to $\bar{X}+1.0\ \sigma$ value (100 ppm). This value was used as the threshold value.

Hg: About 67% of the cells contained amount below detection limit values, thus the cumulative frequency curve is out of the logarithmic normal dispersion, but the inflection point is still observed at 95% which corresponds to 800 ppb.

Cr: The curve showed inflection point at 90% which corresponds to values the between $\bar{X}+1.0\ \sigma$ value and $\bar{X}+1.5\ \sigma$ value (40,000 ppm). This value was used as the threshold value.

3-2-1-2-3 Correlation coefficients between each element

Correlation coefficients between each element are shown on Table-11 and Table -12.

Table-11 Correlation coefficients (between Elements) in of Cell Average Values (Southern Part)

	Cu	Pb	Zn	Ag	As	Mn	Ni	Co	Mo	Hg	Cr
Cu	1.000										
Pb	−0.011	1.000									
Zn	0.635	0.250	1.000								
Ag	—	—	—	1.000							
As	−0.162	0580	0.164	—	1.000						
Mn	0.600	−0.002	0.701	—	−0.141	1.000					
Ni	0.231	−0.395	0.272	—	−0.443	0.621	1.000				
Co	0.391	−0.382	0.376	—	−0.487	0.741	0.928	1.000			
Mo	—	—	—	—	—	—	—	—	1.000		
Hg	0.005	0.173	0.166	—	0.261	0.066	−0.033	−0.096	—	1.000	
Cr	0.055	−0.470	0.022	—	−0.466	0.393	0.887	0.788	—	−0.126	1.000

Table-12 Correlation Coefficients (between Elements) in the Original Analyses (Southern Part)

	Cu	Pb	Zn	Ag	As	Mn	Ni	Co	Mo	Hg	Cr
Cu	1.000										
Pb	0.004	1.000									
Zn	0.576	0.259	1.000								
Ag	—	—	—	1.000							
As	−0.100	0.541	0.201	—	1.000						
Mn	0.544	0.026	0.660	—	−0.098	1.000					
Ni	0.198	−0.375	0.249	—	−0.441	0.597	1.000				
Co	0.350	−0.342	0.327	—	−0.456	0.707	0.910	1.000			
Mo	—	—	—	—	—	—	—	—	1.000		
Hg	0.033	0.136	0.189	—	0.216	0.101	−0.013	−0.067	—	1.000	
Cr	0.040	−0.441	−0.013	—	−0.459	0.362	0.860	0.752	—	−0.110	1.000

In the cell average values, positive correlations are observed among the following elements.

Cu-Zn, Mn Pb-As, Zn-Mn, Mn-Ni, Co Ni-Co, Cr Co-Cr,

3-2-1-2-4 Areal distribution of the cell average values (Attached plate 2-1-2 No.1 - No. 10)

The cell average values of each element are classified into 11 ranks and plotted in a 1:1,000,000 scale areal map with corresponding rank colors.

Classified ranges are as follows.

Code	Cumulative frequency range
A	99% ≦ Z
B	95% ≦ Z < 99%
C	90% ≦ Z < 95%
D	75% ≦ Z < 90%
E	60% ≦ Z < 75%
F	50% ≦ Z < 60%
G	40% ≦ Z < 50%
H	30% ≦ Z < 40%
I	20% ≦ Z < 30%
J	Detection limit ≦ Z < 20%
K	Detection limit ≦ Z

The areal distribution of the anomalous cell average values of each element are as follows:

East side of Ulugan Bay.
(Anomalous elements; Ni, Co, and Cr)

Northern part of Puerto Princesa
(Anomalous elements; Cu, Zn, Mn, Hg and Cr)

Vicinity of Long Point in the west coast.
(Anomalous elements; Zn, Mn, Ni, Co. and Cr)

Vicinity of Moorsom Point in the west coast.
(Anomalous elements; Zn As, Mn, Ni, Co and Cr)

Panacan to Victoria Peak in the east coast.
(Anomalous element; Ni, Co and Cr)

North side of Aboabo
(Anomalous elements; Zn, As and Mn)

South side of Aboabo to Pulute Range.
(Anomalous elements; Cu, Pb, Zn, As, Mn and Hg)

Vicinity of Barong-Barong in the southwestern part.
(Anomalous elements; Cu, Zn, Mn and Co)

Northeastern part of Rio Tuba
(Anomalous elements; Cu and As)

Vicinity of Escapard Peak in northern part of Rio Tuba.
(Anomalous elements; Cu, Zn, As, Mn, Ni, Co and Cr)

East coast of Balabac Island
(Anomalous elements; Cu, Zn, As and Mn)

The following four zones can be explained by their respective geological settings, igneous activities and mineralizations.

(a) Northern part of Puerto Princesa: Overthrusted ultramafic rocks and Cretaceous basement rocks are distributed in this zone and Post-Miocene hydrothermal mineralization is also know. The anomalous values of Ni, Co, Cr and Mn are assumed to have been derived from these country rocks. The Hg anomaly is probably related to the Neogene mineralization event.

(b) The area from Long Point in the west coast to Panacan in the southeastern coast: Mt. Beaufort Ultramafics is distributed in this zone and several Ni and Cr mineral showings are known. Anomalous values of Ni, Co and Cr are assumed to have been derived from the ultramafic country rocks.

(c) Vicinity of the southwestern mountain range: Overthrusted ultramafics and Cretaceous basement rocks are distribute in this zone and nickel laterite and Cyprus type massive sulfide mineral showings are known to exist. The anomalous values of various elements are assumed to have been derived from these lithological formations.

(d) East-central coast of Balabac Island: The basement, the Espina Basalt, is distributed in this zone and Cyprus type mineral showings is known to exist. The anomalous values are assumed to have been derived from this rock.

3-2-1-3 Moving Average Values of the Northern Part

The average value of the nine cells (three cells respectively both in NS and EW directions) is supposed to be the value of the central cell. This average value is called the moving average value of the cell.

The gap filling procedure to a blank cell at the edge is done in such a way that when there are effective values in three cells among the five cells which enclose the blank cell in an embayed shape, the average value of these three values is taken as the moving average value of the embayed blank cell. This gap filling procedure has been done twice.

3-2-1-3-1 Basic statistical values

Moving average procedure was applied to 1,667 cell average values and the basic statistical values were calculated. Details are shown in Table-13.

3-2-1-3-2 Histograms and cumulative frequency curves

Histograms and cumulative frequency curves which show dispersion of the moving average values are presented separately for each element. The range of anomalous values were determined

Table-13 Basic Statistical Values of Moving Average Values (Northern Part)

	Cu (ppm)	Pb (ppm)	Zn (ppm)	Ag (ppm)	As (ppm)	Mn (ppm)	Ni (ppm)	Co (ppm)	Mo (ppm)	Hg (ppb)	Cr (ppm)	Sb (ppb)	Sn (ppm)	W (ppm)
$\bar{X}$	8.00	5.88	23.11	0.50	3.56	167.68	7.69	3.82	1.00	26.98	70.46	117.01	0.52	1.53
$\bar{X}+1.0\sigma$	13.63	7.27	40.95	0.50	6.71	315.59	14.64	6.46	1.00	40.43	118.23	236.99	0.61	1.64
$\bar{X}+1.5\sigma$	17.74	8.09	54.52	0.50	9.21	432.96	20.20	8.40	1.00	49.50	153.15	337.26	0.66	1.70
$\bar{X}+2.0\sigma$	23.13	9.00	72.59	0.50	12.64	593.97	27.87	10.93	1.00	60.60	198.39	479.96	0.72	1.76
Minimum	1.08	5.00	1.79	0.50	0.31	25.17	1.50	1.50	1.00	20.00	50.00	25.00	0.50	1.50
Maximum	31.11	14.79	72.42	0.50	34.56	1,093.10	345.61	28.39	1.00	129.95	7,855.60	1,218.10	4.35	3.04
Number of cell	1,610	1,610	1,610	1,610	1,610	1,609	1,609	1,609	908	1,610	1,610	1,610	1,261	1,261
R.B.D.	1.9%	97.2%	0%	100%	0.3%	4.3%	5.7%	35.9%	100%	84.7%	83.6%	11.9%	99%	99.9%

$\bar{X}$: Mean value σ : Standard deviation R.B.D. : Ratio of below detection limit value

by studies on these data.

The anomalous ranges of each element are as follows:

Cu: The curve showed the inflection point at 93% which corresponds to the $\overline{X}+1.5\ \sigma$ value (17.7 ppm). This value was used as the threshold value.

Pb: About 97% of the cells contained amount below detection limit values, thus the cumulative frequency curve was out of the logarithmic normal dispertion. However the inflection point was still observed at 99% cumulative frequency.

Zn: The curve showed inflection point 96% which corresponds to the values between $\overline{X}+1.0\ \sigma$ and $\overline{X}+1.5\ \sigma$ value (48 ppm). This value was used as the threshold value.

As: The curve showed inflection point at 96% which corresponds to the value $\overline{X}+1.5\ \sigma$ value (10 ppm). This value was used as the threshold value.

Mn: The curve showed inflection point at 96% which corresponds to the values between $\overline{X}+1.5\ \sigma$ and $\overline{X}+2.0\ \sigma$ value (500 ppm). This value was used as the threshold value.

Ni: The curve showed inflection point at 95% which corresponds to the $\overline{X}+1.5\ \sigma$ value (300 ppm). This value was used as the threshold value.

Co: The curve showed inflection point at 79% cumulative frequency which corresponds to $\overline{X}+1.0\ \sigma$ value (5 ppm). This value was used as the threshold value.

Mo: All of the cells contained amount below detection limit values. So the Mo was omitted from statistical analysis.

Hg: 85% of the cells contained amount below detection limit value. The inflection point is still observed at 96% cumulative frequency.

Cr: About 84% of the cells contained amount below detection limit values, but the cumulative frequency curve shows inflection point at 94% cumulative frequency which corresponds to values between $\overline{X}+1.5\ \sigma$ and $\overline{X}+2.0\ \sigma$ value (180 ppm). This value was used as the threshold value.

Sb: The curve showed inflection point at 98% which corresponds to $\overline{X}+2.0\ \sigma$ value (580 ppb). This value was used as the threshold value.

Sn: About 99% of the cells contained amount below detection limit values, thus the range of the anomalous values was unclear.

W: About 99.9% of the cells contained amount below detection limit values, thus the range of the anomalous values was not clear.

3-2-1-3-3 Areal distribution of the moving average values (Attached plate 2-2-1 No.1 - No. 12)

The moving average values of each element are classified into 11 ranks and plotted in a 1:1,000,000 scale map with corresponding rank colors.

Classified ranges are as follows.

Code	Range	Code	Range
A	$99\% \leqq Z$	F	$50\% \leqq Z < 60\%$
B	$95\% \leqq Z < 99\%$	G	$40\% \leqq Z < 50\%$
C	$90\% \leqq Z < 95\%$	H	$30\% \leqq Z < 40\%$
D	$75\% \leqq Z < 90\%$	I	$20\% \leqq Z < 30\%$
E	$60\% \leqq Z < 75\%$	J	Detection limit $< Z < 20\%$
		K	Detection limit $< Z$

The anomalous zones with their corresponding elements are as follows:

Eastern part of Busuanga Island (Cu, Zn, As, Mn, Ni, Co, Hg, Cr, and Sb).

South-central part of Busuanga Island (Cu, Mn, Ni, Co, Cr and Sb).

East coast of Culion Island (Cu, Mn and Hg).

Northeastern part of Pancol (Cu, Zn, Mn, Ni, Co and Hg).

Maytiguit Island offshore NE of Main Palawan Island (Cu, Mn, Ni, Co and Hg).

Northwestern part of Taytay (Cu, Zn, Mn, Ni, Hg and Cr).

Vicinity of Mt. Kapoas (Sn).

Northwestern part of Tinitian (As and Sb).

East side of St. Paul Pay (Pb and Zn).

East side of Ulugan Bay (Zn, Mn, Ni, Co, Hg, Cr and Sb).

These anomalous zones are showing in a larger scale than the cell average values, as a result of the smoothing. The anomalies of the following five zones can be explained by their respective geological settings, igneous activities and mineralizations:

(a) Eastern part of Busuanga Island: Paleozoic and Mesozoic sedimentary rocks are distributed in this zone and strata-bound manganese mineral showings are known to exist. Since no mineralization or igneous activity is known over the area, the overlapping various elements except Mn are inferred to have derived by some other mechanism besides mineralization (for example; absorption of pelitic sediments.)
The elements which show the concentration of anomalous cells are same that of cell average values.

(b) Northwestern part of Pancol in the northwestern part of main Palawan Island: Permian sedimentary rocks and Jurrassic cherty rocks are distributed in this zone. Mineralization is unknown but the overlapping anomalous values of various elements suggest the existence of mineralization which is

associated with the diorite intrusions.

The elements which show the concentration of anomalous cells are added As with compare to that of cell average values.

(c) The vicinity Mt. Kapoas: This anomalous zone is located at the periphery of the Kapoas Diorite stocks and is composed only of Sn anomalous cells same that of cell average values. This anomaly is inferred to be related to the Kapoas Diorite.

(d) The northwestern part of Tinitian in the eastern coast: The Caramay Schist is distributed in this zone and antimony mineralization associated with quartz veins is observed. As and Sb anomalous values are assumed to have originated from these quartz veins, these anomalous elements are same to that of call average values.

(e) East side of Ulugan Bay in Central Palawan: The Sabang Thrust which divides the Northern and Southern Part passes at the west side of this anomalous zone. The ultramafic rocks are exposed along the west side of the thrust. Ni, Co and Cr overlapping anomalies are assumed to be related to these ultramafics. Hg anomalous values are assumed to reflect the presence of hydrothermal mineralization which has been noted to exist in the central Palawan area.

The addition a elements which show the concentration of anomalous cells are Zn and Sb as compare with cell average values.

3-2-1-4 Moving Average Values of the Southern Part

The procedure followed here is basically similar to what has been done for the Northern Part.

3-2-1-4-1 Basic statistical values

Moving average procedure was applied to 1,623 cell average values and the basic statistical values were calculated. Details are shown in Table-14.

3-2-1-4-2 Histograms and cumulative frequency curves

Histograms and cumulative frequency curves which show the dispersion of the moving average values are presented separately for each element.

The range of anomalous values were determined by studies on these data.

The anomalous ranges of each element are as follows:

Cu: The curve showed the inflection point at 79% which corresponds to the $\overline{X}+1.0\,\sigma$ value (37 ppm). This value was used as the threshold value.

Pb: About 93% cells contained amount below detection limit values, thus the curve was out of the logarithmic normal dispertion. The inflection point, however, was still observed at 95%.

Zn: The curve showed inflection point at 94% which corresponds to the values $\overline{X}+1.5\,\sigma$ value (70 ppm). This value was used as the threshold value.

As: The curve showed inflection point at 90% which corresponds to the $\overline{X}+1.5\,\sigma$ value (40 ppm). This value was used as the threshold value.

Mn: The curve showed inflection point at 97% which corresponds to the $\overline{X}+2.0\,\sigma$ value (2,000 ppm). This value was used as the threshold value.

Ni: The curve showed inflection point at 88% which corresponds to the values between $\overline{X}+1.0\,\sigma$ and $\overline{X}+1.5\,\sigma$ value (1,900 ppm). This value was used as the threshold value.

Co: The curve showed inflection point at 90% which corresponds to $\overline{X}+1.0\,\sigma$ value (100 ppm). This value was used as the threshold value.

Hg: About 64% cells contained amount below detection limit values. The inflection point is observed at 96% cumulative frequency which corresponds to 900 ppb. This value was used as the threshold value.

Cr: The curve showed inflection point at 91% which corresponds to the values between $\overline{X}+1.0\,\sigma$ and $\overline{X}+1.5\,\sigma$ value (30,000 ppm). This value was used as the threshold value.

3-2-1-4-3 Areal distribution of the moving average values (Attached Plate 2-2-2 No.1~No.9)

The moving average values of each element are classified into 11 ranks and plotted in a 1:1,000,000 scale map with each corresponding rank colors:

Table-14 Basic Statistical Values of Moving Average Values

	Cu (ppm)	Pb (ppm)	Zn (ppm)	Ag (ppm)	As (ppm)	Mn (ppm)	Ni (ppm)	Co (ppm)	Hg (ppb)	Cr (ppm)
$\overline{X}$	21.31	6.04	44.68	0.50	0.95	643.98	223.31	31.96	40.58	3,108.31
$\overline{X}+1.0\,\sigma$	38.33	7.90	64.19	0.50	2.26	1,110.61	1,031.18	78.11	101.67	20,823.47
$\overline{X}+1.5\,\sigma$	51.41	9.04	76.95	0.50	3.48	1,458.50	2,215.87	122.12	160.93	53,897.30
$\overline{X}+2.0\,\sigma$	68.95	10.34	92.24	0.50	5.37	1,915.34	4,761.51	190.94	254.72	139,502.18
Minimum	1.79	5.00	5.43	0.50	0.25	41.08	2.32	1.66	20.00	50.00
Maximum	66.03	16.29	129.25	0.50	7.03	2,256.30	5,521.30	301.98	6,131.10	97,411.00
Number of cell	1,616	1,535	1,616	1,616	1,616	1,616	1,616	1,535	1,616	1,535
R.B.D.	0%	92.8%	0%	100%	30.2%	0%	0%	0.7%	63.8%	5.2%

$\overline{X}$: Mean value σ : Standard deviation R.B.D. : Ratio of below detection limit value

Classified ranges are as follows.

Code	Range	Code	Range
A	99% ≦ Z	F	50% ≦ Z < 60%
B	95% ≦ Z < 99%	G	40% ≦ Z < 50%
C	90% ≦ Z < 95%	H	30% ≦ Z < 40%
D	75% ≦ Z < 90%	I	20% ≦ Z < 30%
E	60% ≦ Z < 75%	J	Detection limit < Z < 20%
		K	Detection limit < Z

The different anomalous zones with their corresponding elements are as follows:

East side of Ulugan Bay (Ni, Co and Cr).

North and west side of Puerto Princesa (Cu, Zn, Mn, Ni and Hg).

West coast of Long Point to Moorsom Point (Cu,Zn, Mn, Ni,Co and Cr).

North side of Aboabo in the south coast (Cu, Zn and Mn).

Southwestern part of Aboabo (Pb, Mn and Hg).

North side of Barong-Barong in the southern part (Zn, Mn, Ni and Co).

Vicinity of Spike Peak (Pb, As and Hg).

North and northeastern part of Rio Tuba (Cu, Zn, As, Mn, Ni and Co).

East-central part of Balabac Island (Cu, Zn and Mn).

These anomalous zones are shown in a larger scale than the cell average values, as a result of the smoothing. The following seven zones can be explained by their respective geological settings, igneous activities and mineralizations:

(a) East side of Ulugan bay: Northern part of the overthrusted ultramafic rocks is distributed in this zone. The Ni, Co and Cr anomalous values are assumed to have been derived from these ultramafic rocks. The anomalous elements are same to that of cell average values.

(b) Northern part of Puerto Princesa: In this zone, overthrusted ultramafic rocks and Cretaceous basement complex are distributed and Post-Miocene hydrothermal mineral showings are known to exist. Anomalies of various elements were derived from these different geological settings. As compare with cell average values, Cr anomalous cells are missing and Ni anomaleous cells are including to this zone.

(c) West coast zone from Long Point to Moorsom Points: Overthrusted ultramafic rocks and basement formation are distributed in this zone. Lenticular chromite and nickel laterite mineral showings are known. Ni, Co and Cr anomalies are associated with the ultramafic rocks while the Cu, Zn and Mn anomalies reflect the influence of the basement formation. As compare with cell average values.

(d) Vicinity of Aboabo in the southern coast: Overthrusted ultramafic rocks and basement complex are distributed in this zone. As anomalous cells are missing from this zone at the vicinity of Moorsom Point in the western coast.
Ni and Co anomalies again are associated with the ultramafic rocks while the Cu, Zn and Mn anomalies are related to the of basement complex. As compare with cell average values, Cu, As and Zn anomalous cells are missing from the anomalous zone at south side Aboabe in the central part..

(e) North side of Barong-Barong in the southwestern part: In this zone, overthrusted ultramafic rocks and Cretaceous basement rocks are distributed and Cyprus type copper mineral showings are known to occur. Ni and Co anomalies were derived from the ultramafic rocks and Zn and Mn anomalies are associated with the basement rocks. As compare with cell average values, Cu anomalous cells are missing and Ni anomalous cells are containing to this zone..

(f) The vicinity of Rio Tuba: In this zone, Cretaceous basement rocks, Tertiary sediments and overthrusted ultramafic rocks are observed. Nickel laterite is being mined at present by the Rio Tuba Mine. Anomalies of various elements would have been derived from this geological setting. As compare with cell average values, Cr anomalous cells are missing from this zone.

(g) East coast of Balabac Island: In this zone, Cretaceous basement rocks and overthrusted ultramafic rocks are observed and Cyprus type copper mineralization is known to exist (Balabac Mine: suspended). Cu, Zn and Mn anomalies is believed to have resulted from this mineralization. The anomalous zone shows a little deviation to the south from the mine site. As compare with cell average values, As anomalous cells are missing from this zone.

Table-15 Basic Statistical Values of High-pass Filter Values (Northern Part)

	Cu(ppm)	Pb(ppm)	Zn(ppm)	Ag(ppm)	As(ppm)	Mn(ppm)	Ni(ppm)	Co(ppm)	Mo(ppm)	Hg(ppb)	Cr(ppm)	Sb(ppb)	Sn(ppm)	W(ppm)
$\overline{X}$	1.82	1.39	4.40	0.46	1.21	44.92	2.22	1.43	——	6.53	17.91	32.35	0.46	1.26
$\overline{X}+1.0\sigma$	6.69	4.42	18.06	0.46	4.36	241.20	9.65	4.64	——	38.42	158.42	153.27	1.28	5.27
$\overline{X}+1.5\sigma$	12.85	7.89	36.61	0.46	8.30	558.94	20.11	8.37	——	93.19	471.18	333.63	2.13	10.77
$\overline{X}+2.0\sigma$	24.67	14.08	74.19	0.46	15.78	1,295.24	41.91	15.11	——	226.06	1,401.45	726.23	3.55	22.03
Minimum	0.10	0.10	0.10	0.46	0.10	0.14	0.10	0.11	——	0.10	0.10	0.14	0.14	0.12
Maximum	79.26	15.36	147.60	0.46	75.95	6,314.90	2,062.20	119.09	——	1,143.00	20,720.00	6,130.20	11.25	31.00
Number of cell	710	286	754	1	657	755	698	615		353	409	748	40	19

$\overline{X}$; Mean value σ ; Stabndard deviation

3-2-1-5 High Pass Filter Values of the Northern Part

High pass filter value is the positive difference between the moving average value and from the cell average value.

The deduction procedure aims to correct the local back-ground value which is indicated by the moving average value.

Therefore, high-pass filter value directly indicates anomalous zones which were derived from latter added factors such as mineralization, secondary enrichment and others, and provides guideline to the locality, intensity and priority of the geochemical anomalous zones.

3-2-1-5-1 Basic statistical values

Basic statistical values are calculated from the cell average values and moving average values of each element, the details, of which are shown in Table-15.

3-2-1-5-2 Histograms and cumulative frequency curves

Histograms and cumulative frequency curves which show the dispersion of the high-pass filter values are presented separately for each element.

The range of anomalous values were determined by studies on these data.

The anomalous ranges of each element are as follows.

Cu: The curve showed the inflection point at 96% which corresponds to values between $\overline{X}+1.5\,\sigma$ and $\overline{X}+2.0\,\sigma$ value (19 ppm). This value was used as the threshold value.

Pb: The curve showed inflection point at 90% which corresponds to values between $\overline{X}+1.0\,\sigma$ and $\overline{X}+1.5\,\sigma$ value (6 ppm). This value was used as the threshold value.

Zn: The curve showed inflection point at 92% cumulative frequency which corresponds to the values between $\overline{X}+1.0\,\sigma$ and $\overline{X}+1.5\,\sigma$ (28 ppm). This value is used as the threshold value.

As: The curve showed inflection point at 96% which corresponds to the values between $\overline{X}+1.0\,\sigma$ and $\overline{X}+1.5\,\sigma$ (10 ppm). This value was used as the threshold value.

Mn: The curve showed inflection point at 90% which corresponds to values between $\overline{X}+1.0\,\sigma$ and $\overline{X}+1.5\,\sigma$ (400 ppm). This value was used as the threshold value.

Ni: The curve showed inflection point at 90% which corresponds to the values between $\overline{X}+1.0\,\sigma$ and $\overline{X}+1.5\,\sigma$ (15 ppm). This value was used as the threshold value.

Co: The curve showed inflection point at 90% which corresponds to values between $\overline{X}+1.0\,\sigma$ and $\overline{X}+1.5\,\sigma$ (6 ppm). This value was used as the threshold value.

Mo: All cells did not show effective high-pass filter value, thus, Mo values were omitted from the analysis.

(I) Hg: The curve showed inflection point at 99% which corresponds to more than $\overline{X}+2.0\,\sigma$ value (350 ppm). This value was used as the threshold value.

(J) Cr: The curve showed inflection point at 97% which corresponds to more than $\overline{X}+2.0\,\sigma$ value (2,500 ppb). This value was used as the threshold value.

(K) Sb: The curve showed inflection point at 93% which corresponds to values between $\overline{X}+1.0\,\sigma$ and $\overline{X}+1.5\,\sigma$ (200 ppb). This value was used as the threshold value.

(L) Sn: The curve showed inflection point at 90% which corresponds to value between $\overline{X}+1.5\,\sigma$ and $\overline{X}+2.0\,\sigma$ (2.8 ppm). This value was used as the threshold value.

(M) W: The curve showed inflection point at 90% which corresponds to value between $\overline{X}+1.5\,\sigma$ and $\overline{X}+2.0\,\sigma$ (7 ppb). This value was used as the threshold value.

3-2-1-5-3 Areal distribution of high pass filter anomalous values (Attached plate 2-3-1 No.1 - No. 12)

The anomalous value is classified based on the following formula, with each element plotted on a 1:1,000,000 scale map with the corresponding different color-red, yellow and blue.

Table-17 High Pass Filter Value Dlassification Formula

Rank	Classification formula	Color
A	$\overline{X}+2.0\,\sigma < Z$	Red
B	$\overline{X}+1.5\,\sigma < Z < \overline{X}+2.0\,\sigma$	Yellow
C	$\overline{X}+1.0\,\sigma < Z < \overline{X}+1.5\,\sigma$	Blue

The anomalous zones which are strongly related to the high rank cells of the cell average value are as follows:

East-central part of Busuanga Island (Cu, Zn, As, Mn, Ni, Co, Cr and Sb).

Southeastern part of Culion Island (Cu, Mn, Ni, Co, Cr and Sb).

The east side of El Nido to Mt. Kapas (Cu, Zn,As, Mn, Ni, Hg, Sb and Sn).

Southeastern part of Taytay (Cu, Zn, Mn, Ni, Co, Hg and Cr).

Around part of Big Peak (Pb, As, Co and W).

Northern part of Taradungan (Cu, Pb, Zn, As, Ni, Hg, Sb and W).

Northwestern part of Tinitian (As, Sb and Cr).

Western part of the Central Range (Pb, As and Co).

The following three zones can be explained by their respective geological settings, igneous activities and mineralizations:

(a) Eastern and south-central part of Busuanga Island: In this zone, Paleozoic and Mesozoic sedimentary rocks are distributed and strata-bound Mn mineral showings are known to occur.
Other mineralization, mineral showings and basic or ultrabasic igneous activity are unknown. From these geological setting, the overlapping anomalies of the various elements except manganese is inferred to have derived from some other mechanism besides mineralization(for example, absorption by pelitic sediments). As compare with the anomalous zone of cell average values, As anomalous cells are missing form this anomalous zone.

(b) Zone of the east side of El Nido to Mt. Kapoas: In this zone, Kapoas diorite stocks intruded in a NNE - SSW direction. Mineral showings are unknown, but the combination of the anomalous elements suggests the existence of mineralization associated with the diorite intrusion.
As compare with the anomalous zone of cell average values, Co anomalous cells are missing and Sb and Sn anomalous cells are containing to this anomalous zone.

(c) Northwestern part of Tinitian: In this zone, antimony mineral showings are known. The As and Sb anomalies would have been derived from these showings.
As compare with the anomalous zone of cell average values, Cr anomalous cells are containing to this zone.

3-2-1-6 High Pass Filter Values of the Southern Part

3-2-1-6-1 Basic statistical values

Basic statistical values are calculated from the cell average values and moving average values of each element, the details, of which are shown in Table-16.

3-2-1-6-2 Histograms and cumulative frequency curves

Histograms and cumulative frequency curves which show dispersion of the high-pass filter values are presented separately for each element.

The range of anomalous values were determined by studies on these data.

The anomalous ranges of each element are as follows.

Cu: The curve showed inflection point at 98% which corresponds to values between $\overline{X}+1.5\ \sigma$ and $\overline{X}+2.0\ \sigma$ (35 ppm). This value was used as the threshold value.

Pb: The curve showed inflection point at 93% which corresponds to values between $\overline{X}+1.0\ \sigma$ and $\overline{X}+1.5\ \sigma$ (8 ppm). This value was used as the threshold value.

Zn: The curve showed inflection point at 92% which corresponds to values between $\overline{X}+1.0\ \sigma$ and $\overline{X}+1.5\ \sigma$ (20 ppm). This value was used as the threshold value.

As: The curve showed inflection point at 90% which corresponds to values between $\overline{X}+1.0\ \sigma$ and $\overline{X}+1.5\ \sigma$ (2 ppm). This value was used as the threshold value.

Mn: The curve showed inflection point at 92% which corresponds to values between $\overline{X}+1.0\ \sigma$ and $\overline{X}+1.5\ \sigma$ (580 ppm). This value was used as the threshold value.

Ni: The curve showed inflection point at 90% which corresponds to the values between $\overline{X}+1.0\ \sigma$ and $\overline{X}+1.5\ \sigma$ (100 ppm). This value ws used as the threshold value.

Co: The curve showed inflection point at 96% which corresponds to values between $\overline{X}+1.5\ \sigma$ and $\overline{X}+2.0\ \sigma$ (90 ppm). This value was used as the threshold value.

Hg: The curve showed inflection point at 87% which corresponds to value between $\overline{X}+1.0\ \sigma$ and $\overline{X}+1.5\ \sigma$ (300 ppb). This value was used as the threshold value.

Cr: The curve showed inflection point at 95% which corresponds to values between $\overline{X}+1.0\ \sigma$ and $\overline{X}+1.5\ \sigma$ (30,000 ppm). This value was used as the threshold value.

3-2-1-6-3 Areal distribution of high pass filter anomalous values (Attached plate 2-3-1 No.1 - No. 9)

Each anomalous value is classified based on the following standard, with each element plotted on a 1:1,000,000 map with the corresponding different color-red, yellow and blue as similar to the Northern Part.

The anomalous zones which are strongly related to the high rank cells of the cell average value are as follows:

Northern part of Puerto Princesa (Cu, Zn and Hg)

Table-16 Basic Statistical Values of High-pass Filter Values (Southern Part)

	Cu(ppm)	Pb(ppm)	Zn(ppm)	Ag(ppm)	As(ppm)	Mn(ppm)	Ni(ppm)	Co(ppm)	Hg(ppb)	Cr(ppm)
$\overline{X}$	3.24	1.54	4.15	–	0.54	84.02	71.27	4.97	15.32	1,296.40
$\overline{X}+1.0\ \sigma$	12.67	5.69	15.99	–	1.46	384.31	586.53	26.07	182.87	16,,383.13
$\overline{X}+1.5\ \sigma$	25.06	10.93	31.39	–	2.42	821.94	1,682.57	59.71	616.86	58,240.49
$\overline{X}+2.0\ \sigma$	49.55	20.99	61.65	–	3.99	1,757.88	4.826.74	136.74	2,183.50	207,039.40
Minimum	0.10	0.10	0.10	–	0.10	0.27	0.11	0.10	0.13	0.14
Maximum	158.77	23.58	98.54	–	21.38	3,276.90	743.10	743.10	25,205.00	118,370.00
Number of cell	788	289	798		520	781	799	738	472	761

$\overline{X}$: Mean value σ ; Standard deviation

Triple Top Range in the southern part of Puerto Princesa (Cu, Zn, Co and Hg)

Surrounding area of Long Point to Moorsom Point in the west coast (Cu, Zn, As, Ni and Co).

Around Birong in the west coast (Mn, Ni, Hg and Cr).

West side of Quezon (Zn and As).

Around Panacan in the east coast (As and Cr).

North side of Barong-Barong (Cu, Mn, Ni and Co).

Northwestern part of Mt. Mantalingajan (Pb and As).

Northern and northeastern part of Rio Tuba (Cu, Pb, Zn, As, Mn, Ni and Co).

The anomalous zones of the following four zones can be explained by their respective geological settings, igneous activities and mineralizations:

(a) Northern part of Puerto Princesa: In this zone, overthrusted ultramafic rocks and Cretaceous basement rocks are distributed and Hg and Sb mineralizations inferred to be associated to Post-Miocene hydrothermal mineralizations are known. Cu, Zn and Hg anomalies are also inferred to this mineralization.
As compare with the anomalous zone of cell average values, Mn and Cr anomalous cells are missing from this anomalous zone.

(b) The vicinity of Long Point to Moorsom Point in the west coast: In this zone, overthrusted ultramafic rocks and Cretaceous basement rocks are distributed and lenticular chromite and nickel laterite mineral showings are known.
Ni, Co anomalies are associated with the ultramafic rocks, while the Cu, Zn and As anomalies are inferred to be related to the basement rocks.
As compare with the anomalous zone of cell average values, Cr anomalous cells are missing and Cu anomalous cell are containing to this anomalous zone.

(c) North side of Barong-Barong: In this area, overthrusted ultramafic rocks and the Cretaceous Espina Basalt are distributed, Cyprus type massive sulfide mineral showings are known. Cu and Mn anomalies are inferred to be related to the Espina Basalt while the Ni and Co anomalies were derived from the ultramafic rocks.
As compare with the anomalous zone of cell average values, Zn anomalous cells are missing and Ni anomalous cells are containing to this anomalous zone.

(d) Northern and northwestern part of Rio Tuba: Overthrusted ultramafic rocks, Cretaceous Espina Basalt, Eocene Panas Formation and Miocene Sayab Formation are distributed, in this zone Rio Tuba has a large nickel laterite deposit which consists of weathered ultramafic rocks.
Cu, Pb, Zn, As and Mn anomalies are inferred to concern be related to the Espina Basalt, while Ni and Co anomalies were derived from the weathered ultramafic rocks.
As compare with the anomalous zone of cell average value, Pb anomalous cells are containing and Cr anomalous cells are missing from this anomalous zone.

3-2-2 Multivariate Analysis (Factor Analysis)

3-2-2-1 Factor Analysis in the Northern Part

Factor analysis was carried out on each cell average values using the Varimax rotation method.

The elements which are below the detection limit value in over 80% of the analyzed sample (Pb, Ag, Mo, Hg, Cr, Sn and W) are excluded from this analysis. The remaining seven elements (Cu, Zn, As, Mn, Ni, Co and Sb) are used for factor analysis is seven.

3-2-2-1-1 Correlation analyses

At first, the correlation matrix (Table-18) between each element of the cell average values were solved, then the eigen values and cumulative proportions of total variances were calculated.

Table-18 Correlation Matrix and Eigen Values (Nothern Part)

	Cu	Zn	As	Mn	Ni	Co	Sb
Cu	1.000						
Zn	0.719	1.000					
As	0.444	0.415	1.000				
Mn	0.749	0.737	0.420	1.000			
Ni	0.697	0.745	0.265	0.731	1.000		
Co	0.710	0.681	0.322	0.803	0.812	1.000	
Sb	0.251	0.080	0.492	0.225	0.118	0.180	1.000
	Factor No.1	Factor No.2	Factor No.3	Factor No.4	Factor No.5	Factor No.6	Factor No.7
Eigen Value	4.250	1.265	0.537	0.298	0.278	0.230	0.143
(Diagonal factor: 1)							
C.P.T.V.	0.607	0.788	0.865	0.907	0.947	0.980	1.000
Eigen Value	3.942	0.861	0.101	−0.012	−0.057	−0.105	−0.220
(Diagonal factor: S.M.C.)							

C.P.T.V.: Cumulative Proportion of Total Variance
S.M.C.: Squared Multiple Correlation

It is clear that the cumulative proportion of total variance reaches 90.7% up to the fourth factor of diagonal factor: 1. This means that the great portion of dispersion of each value is covered up to the fourth factor of diagonal factor: 1. On the other hand, the SMC (SMC; squared multiple correlation) diagonal factor is used on the correlation matrix, then another set of eigenvalues were calculated, these eigenvalues show positive values up to the No. 3 factor, but the eigenvalue of fourth factor is very close to 0. From the abovementioned items, up to fourth factors were adopted for the factor analysis.

3-2-2-1-2 Interpretation of each factor

Four factors (Factor No. 1 to No. 4) are adopted and used on the factor analysis. The left half of Table-19 shows factor loadings which were processed by the main factor analysis method (before Varimax rotation).

The right half of Table-19 shows the factor loadings derived after the Varimax rotation.

Table-19 Factor Loading befor and after Rotation

Before Varimax rotation					After Varimax rotation					
Factor	1	2	3	4	Factor	1	2	3	4	Final Communality
Cu	0.876	−0.009	0.027	0.411	Cu	0.471	−0.138	0.181	−0.767	0.965
Zn	0.860	−0.181	0.247	0.113	Zn	0.440	0.053	0.259	−0.352	0.942
As	0.552	0.649	0.477	−0.180	As	0.146	−0.275	0.924	−0.139	0.988
Mn	0.902	−0.075	−0.047	−0.057	Mn	0.773	−0.063	0.251	−0.424	0.882
Ni	0.865	−0.268	−0.161	−0.132	Ni	0.744	−0.075	0.011	−0.145	0.920
Co	0.882	−0.180	−0.212	−0.243	Co	0.905	−0.076	0.114	−0.212	0.935
Sb	0.315	0.837	−0.417	0.069	Sb	0.074	−0.964	0.233	−0.074	0.995

Interpretations of each factor are as follows:

(A) Factor No. 1

Before rotation, the factor loadings show the positive values. It is clear on the correlation matrix (Table-18) that this factor indicates similarity of the each elemount.

After rotation, factor loadings show the same manner as the before rotation.

(B) Factor No. 2

Before rotation, the factor loading values show visible positive values on Sb and As. On the other hand, these elements show visible negative values after rotation. Sb and As have the strong tendency to associate sedimentary rocks, so Factor 2 is inferred to indicate the distribution of the sedimentary rocks or Sb mineralization and its accompanying alteration patterns.

(C) Factor No. 3

The factor loadings of As, Zn and Cu before rotations show positive values. While that of Sb, Co, Ni and Mn show negative values. Although interpretation of the element distribution Factor No. 3 seems to be hardly significant, it is inferred to indicate Zn mineralization and associated alterations due to the high values of Zn and As.

After rotation, all elements show positive values, with the As registering a high value. The As high value in after rotation corresponds to the strong halo associated to mineralization, Factor 3 is inferred to indicate the halo or alteration associated to As mineralization.

(D) Factor No. 4

Factor loading values before rotation show positive values on Cu, Zn and Sb, and negative values on Co, As Ni and Mn. Cu shows quite a high positive value. Therefore, Factor No. 4 indicates Cu mineralization before rotation.

Factor loadings after rotation shows each element in negative value, especially Cu, Mn and Zn showing high negative values. From this fact and the tendency of these elements to be concentrated in igneous rocks. On after rotation, Factor 4 is interpreted to indicate Cu, Mn and Zn mineralizations or the distribution area of igneous rocks.

Based on these interpretations, the following factors seem to be important as indicators of mineralizations.

(a) Factor 4 before rotation indicates Cu mineralization.

(b) Factor 2 before rotation indicates Sb mineralization.

(c) Factor 3 after rotation indicates As halo or alteration patterns.

3-2-2-1-3 Classification of the factor scores

The factor score of each cell is calculated by mutiplying the cell average value of each element and the factor score coefficients, summarizing them for every cell. The statistical procedure is carried out on all these factor scores. These factor scores are classified based on the following eight ranks and are plotted on a 1:1,000,000 scale map.

Rank	Cumulative Frequency	Rank	Cumulative Frequency
A	90% ≦Z< 100%	E	30% ≦Z< 50%
B	80% ≦Z< 90%	F	20% ≦Z< 30%
C	70% ≦Z< 80%	G	10% ≦Z< 20%
D	50% ≦Z< 70%	H	0% ≦Z< 10%

3-2-2-1-4 The distribution of the anomalous values

Attached plates 2-4-1 No. 1 - No. 5 show the areal distribution of these anomalous values. The concentrated areas of anomalous values are as follows.

(A) Factor No. 1 (after rotation)

This factor has close relationship Co, Ni, Mn, Cu and Zn.

a) Distribution area of the Panas Formation at the western margine of the Northern Part. (Concentration of A rank cells.)

b) The surrounding area of El Nido, Taytay and Pancol in the northern part of the main Palawan Island (Concentration of A and B rank cells).

c) The eastern part of Busuanga and Culion Islands (Concentration of A and B rank cells).

(B) Factor No. 2 (before rotation)

This factor has close relationship with Sb and As.

a) From Tinitian in the northeastern coast to the northern coast. (Concentration of A and B rank cells.)

b) From Big Peak to Taradungan in the northeastern part of the main Palawan Island (Concentration of A and B rank cells).

c) The vicinity of El Nido at the northern main Palawan Island (Concentration of A and B rank cells).

d) All parts of Busuanga Island and the west coast of Culion Island (Concentration of A and B rank cells).

(C) Factor No. 3 (before rotation)

This factor has close relationship with As and Zn.

a) The northern part of Tinitian in the south coast of the northern main Palawan Island (Concentration of A and B rank cells).

b) From Taradungan of the east coast to Kapoas Peninsula of the west coast in the northern main Palawan Island (Concentration of A and B rank cells).

c) The surrounding part of El Nido in the northern main Palawan Island (Concentration of A and B rank cells).

(D) Factor No. 3 (after rotation)

This factor has close relationship with As, Zn, Mn and Sb.

a) The northern part of Tinitian in the south coast of the northern main Palawan Island (Concentration of A and B rank cells).

b) The surrounding part of Bay Peak at the southern part of Kapoas Peninsula in the northwestern main Palawan Island (Concentration of A and B rank cells).

c) The east side of El Nido in the northern part of the main Palawan Island (Concentration of A and B rank cells).

(E) Factor No. 4 (before rotation)

This factor has close relationship with Cu.

a) From Taytay to Taradungan in the northeast coast of the main Palawan Island (Concentration of A and B rank cells.)

b) The Western part of Busuanga and Culion Islands (Conentration of A and B rank clees).

3-2-2-2 The Factor Analyses in the Southern part

The method of Analyses is the same to the Northern Part.

The elements which show under detection limit values over 65% of the cells (Pb, Ag and Hg) are excluded from this analyses, therefore, the remaining seven elements used for the factor alyses are Cu, Zn, As, Mn, Ni, Co and Cr.

3-2-2-2-1 Correlation Analyses

At first, the correlation matrix (Table-20 Correlation Matrix and Eigen Values) between each element of the cell average values were solved, then the eigen values and cumulative proportion of total variances were calculated.

It is clear from Table-20 that the cumulative proportion of total variance reaches 91.6% up to factor the third with the diagonal factor : 1. On the other hand, when the SMC (Squared Multiple Correlation) diagonal factor is used on the correlation matrix, then another set of eigenvalues were calculated, these eigenvalues show positive values up to factor No. 3.

From abovementioned items, up to factor No. 3 were adopted for the factor analysis.

Table-20 Correlation Matrix and Eigen Values (Southern Part)

	Cu	Zn	As	Mn	Ni	Co	Cr
Cu	1.000						
Zn	0.642	1.000					
As	−0.171	0.198	1.000				
Mn	0.617	0.693	−0.106	1.000			
Ni	0.238	0.237	−0.423	0.600	1.000		
Co	0.391	0.376	−0.488	0.741	0.928	1.000	
Cr	0.056	0.022	−0.466	0.393	0.887	0.788	1.000
Eigen Value	3.792	1.831	0.786	0.246	0.211	0.100	0.034
(Diagonal factor: 1)							
C.P.T.V.	0.542	0.803	0.916	0.951	0.981	0.995	1.000
Eigen Value	3.624	1.523	0.403	0.009	−0.033	−0.054	−0.160
(Diagonal factor: S.M.C.)							

C.P.T.V.: Cumulative Proportion of Total Variance

3-2-2-2-2 Interpretation of each factor

Three factors (Factor No. 1 to Factor No. 3) were adopted and used on the factor analysis. The left half of Table-21 shows factor loadings which were processed by the main factor analysis method (before rotation).

The right half of Table-21 shows the factor loadings derived after the Varimax rotation.

Table-21 Factor Loadings Before and After Rotation (Southern Part)

	Before rotation						After rotation					
Factor	1	2	3	4	5	Factor	1	2	3	4	5	Final Communality
Cu	0.555	0.603	−0.469	0.322	−0.055	Cu	0.062	−0.317	−0.113	−0.921	−0.188	0.9998
Zn	0.512	0.776	0.100	−0.136	0.327	Zn	0.085	−0.886	0.158	−0.360	−0.228	0.9994
As	−0.462	0.547	0.664	0.193	−0.085	As	−0.303	−0.127	0.939	0.092	0.012	0.998
Mn	0.825	0.419	0.096	−0.195	−0.287	Mn	0.399	−0.404	0.011	−0.359	−0.730	0.985
Ni	0.902	−0.309	0.220	0.082	0.021	Ni	0.931	−0.115	−0.157	−0.089	−0.225	0.964
Co	0.963	−0.152	0.066	−0.079	−0.057	Co	0.802	−0.229	−0.279	−0.174	−0.397	0.962
Cr	0.767	−0.522	0.230	0.188	0.101	Cr	0.962	0.039	−0.174	0.012	−0.011	0.958

Interpretation of each factor are as follows.

(A) Factor No. 1

Before rotation, the factor loadings except As show over 0.5 positive values. It is clear on the correlation matrix (Table-20) that this factor indicates the similarity of each element.

After rotation, the factor loadings show the same manner as the before rotation.

(B) Factor No. 2

Before rotation, the factor loading values show positive values on Cu, Zn, As and Mn and negative values on Cr, Ni and Co. From these, the positive value of Factor No. 2 is inferred to indicate Cu, Zn and Mn mineralizations, while the negative values are inferred to suggest Cr, Ni and Co mineralization or the distribution of ultramafic rocks which are associated with Cr, Ni and Co.

After rotation, the factor loadings except Cr show negative values, the values are high on Zn, Mn and Cu and low on Co, As and Ni. Form these, Factor No. 2 is inferred to show the mineralizations of Zn, Mn and Cu or distribution of igneous rocks which are associated with Zn, Mn and Cu.

As mentioned above, Factor No. 2 is interpreted as to indicate Cu, Zn and Mn mineralizations either before or after rotation, but the more desirable simplified structure is obtained from

before rotation values so these values were adopted on the factor analysis.

(C) Factor No. 3

Before rotation, all the elements except Cu show positive values, especially As which has high value, Cu independently shows a high negative value. From this, the negative side of Factor No. 2 is inferred to indicate Cu mineralization.

After rotation, Zn, As and Mn show positive values, especially As expresses high value. From this, the positive side of Factor No. 3 is inferred to indicate the halo or alteration zone of As.

3-2-2-2-3 Classification of factor scores

The factor score of each cell is calculated in a way similar to how it was done for the Northern Part.

These factor scores are classified based on the following eight ranks and are plotted on a 1:1,000,000 scale map.

Rank	Cumulative Frequency	Rank	Cumulative Frequency
A	90% ≦Z< 100%	E	30% ≦Z< 50%
B	80% ≦Z< 90%	F	20% ≦Z< 30%
C	70% ≦Z< 80%	G	10% ≦Z< 20%
D	50% ≦Z< 70%	H	0% ≦Z< 10%

3-2-2-2-4 The distribution of the anomalous values

Attached plates 2-4-2 No. 1 - No. 4 show the areal distribution of these anomalous values. The concentrated areas of anomalous values are as follows.

(A) Factor No. 1 (before rotation)

This factor has close relationship with Cr, Ni and Co. (A and B rank cells)

a) The east side of Ulugan Bay in the middle north coast. (Concentration of A and B rank cells.)

b) The distribution area of ultramafic rocks from Long Point through Moorsom Point in the central north coast to Panacan in the central south coast. (Concentration of A and B rank cells.)

c) The surrounding area of Barong-Barong mineral showings in the Southern Part of the main Palawan Island. (Concentration of A and B rank cells.)

(B) Factor No. 2 (before rotation)

This factor has a close relationship with Cu, Zn and Mn group (A and B rank cells) and Ni, Co and Cr group. (G and H rank cells.)

a) The surrounding area from Aboabo to the surrounding portion of the southwestern mountain range in the main Palawan Islands. (Concentration A and B rank cells.)

b) The eastern side of Ulugaan Bay in the central north coast in the main Palawan Island. (Concentration of G and H rank cells.)

c) The surrounding part of Panacan in the middle south coast in Palawan main Island. (Concentration of G and H rank cells)

(C) Factor No. 3 (before rotation)

This factor has a close relationship with As (A and B rank cells) and Cu (G and H rank cells).

a) The easternside of Ulugan Bay in the central north coast of the main Palawan Island. (Concentration of A and B rank cells.)

b) From Quezon to Aboabo in the central southern part of the main Palawan Island. (Concentration of A and B rank cells.)

c) The surrounding area of Malabungan at the north coast of the main Palawan island. (Concentration of A and B rank cells.)

d) The surrounding area of Rio Tuba in the southern main Palawan Island. (Concentration of A and B rank cells.)

e) The surrounding area of Puerto Princesa in the central main Palawan Island. (Concentration of G and H rank cells.)

f) The northeastern part of Aboabo in the central southern part of the main Palawan Island. (Concentration of G and H rank cells.)

g) The surrounding part of the southwestern part of the central mountain range in the main Palawan Island. (Concentration of G and H rank cells.)

(D) Factor No. 3 (after rotation)

This factor has a close relationship with As.

a) The eastern side of Ulugan Bay in the central north coast of the main Palawan Island. (Concentration of A and B rank cells.)

b) From Quezon to Aboabo in the central southern part of the main Palawan Island. (Concentration of A and B rank cells.)

c) The west slope of Mt. Mantalingajan in the southern main Palawan Island. (Concentration of A and B rank cells.)

d) The surrounded area of Rio Tuba in the southern main Palawan Island. (Concentration of A and B rank cells.)

e) The central eastern part of Balabac Island. (Concentration of A and B rank cells.)

3-3 Analyses for the Heavy Mineral Samples

3-3-1 Univariate Analyses of the Analytical Results of the Panned Samples

A total of 413 panned samples were collected from the Palawan area. Au, Ag and Ga AAS analyses were carried out in PETROLAB. Univariate analyses of these results were done.

Table-22 Basic Statistical Values in Panned Samples

	The Northern Part (177 panned samples)			The Southern Part (236 panned samples)		
	Au (ppb)	Ag (ppb)	Ga (ppm)	Au (ppb)	Ag (ppb)	Ga (ppm)
$\bar{X}$	120	60	1.34	26	55	3.3
$\bar{X}+1.0\sigma$ value	966	123	2.26	118	89	6.6
$\bar{X}+1.5\sigma$ value	2737	176	2.94	250	113	9.4
$\bar{X}+2.0\sigma$ value	7758	251	3.81	529	144	13.2
Maximum	9600	720	5.00	870	430	16.8
Minimum	< 20	< 100	< 2.0	< 20	< 100	< 2.0
D.L.	20	100	2	20	100	2
R.D.L.V.	74%	79%	64%	86%	97%	47%

$\bar{X}$: Mean value σ: Standard deviation
D.L.: Detection Limit
R.D.L.V.: Ratio of Detection Limit Value

Samples having values that are below the detection limit, during the calculation of statistical procedure were assigned values corresponding to 1/2 of the detection limit value of the corresponding element.

The above $\bar{X}+1.0\ \sigma$ values above were plotted based on the following classification utilizing each element symbol on a 1:1,000,000 areal map. (Attached Plates 3-1 and 3-2.)

Rank	Symbol mark
$\bar{X}+2.0\sigma \leqq Z$	◎
$\bar{X}+1.5\sigma \leqq Z \bar{X}+2.0\sigma$	○
$\bar{X}+1.0\sigma \leqq Z \bar{X}+1.5\sigma$	○

3-3-1-1 The Distribution of Anomalous Panned Samples in the Northern Part (Ref.: Attached Plate 3-1)

The locality map of the anomalous values indicates the following tendencies.

(A) The distribution of panned samples having anomalous Au and Ag values are concentrated at the southern and western parts of the Manguao Volcanics in the northeastern part of the main Palawan island.

(B) The distribution of panned samples having anomalous Ga values are concentrated within the distribution area of the Bacuit Formation in the northern main palawan Island.

3-3-1-2 The Distribution of Anomalous Panned Samples in the Southern Part (Ref.: Attached plate 3-2)

(A) Panned samples having anomalous Au and Ag values are distributed within the northern part of Aborlan and the northern part of Narra and are associated with the metamorphosed portion of the Panas Formation. Anomalous values were also noted at the surrounding area of the Pulot mineral showing and the northern part of Rio Tuba etc., associated with the Panas Formation.

(B) Panned samples having anomalous Ga values are distributed along the eastern part of Puerto Princesa and are associated with the Stavely Range Gabbro distribution, within the vicinity of the Pulot mineral showing and with the Panas Formation distribution at the western side of the Pulute Range.

3-3-2 Modal Analyses of the Identified Minerals of the Panned Samples

Fifty panned samples which consist of twenty samples from the Northern Part and thirty samples from the Southern Part, were selected from the 370 panned samples which were collected from the Palawan area, the component minerals of which were identified with binocular microscope in PETROLAB.

Attached Plate-4-1 and 4-2 show each heavy mineral ratio (Wt. %) to the total amount of heavy minerals with the circular graph and the number in the small central circle showing the total heavy mineral ratio (Wt. %) with respect to the whole sample.

The component minerals and their corresponding weight % are shown in Table-23.

A uniform panning procedure was utilized on the whole area, in order to reflect the background value. In doing so, the areas which have low heavy mineral contents, the panned samples sometimes include considerable amount of silicate minerals were included in the panned samples.

3-3-2-1 Specific Nature of the Heavy Mineral Ratios in the Northern Part

They heavy mineral ratios of twenty panned samples collected from the Northern Part are within the range of 0 to 16% except for three samples. This fact is due to the low heavy mineral content of the chert-rich formations such as the Busuanga Chert, etc., which occupy the major part of the area.

One of the exception is a sample collected from Paly Island that showed 92% heavy mineral ratio. The other two exceptional samples were collected from the Caramay Schist and the Concepcion

Table-23 Major Constituent Minerals and Average Wt (%) of the Panned Samples

	Heavy Minerals						Rock Forming Minerals					
Identified Minerals	Magnetite	Chromite	Ilmenite	Rutile	Iron minerals	Zircon	Olvine	Pyroxene	Amphybole	Feldspar	Quartz	Others
Code	mt	cm	il	ru	Fe	Z	ol	P	Ho	F	Q	oth
The Northern Part	0.30%	10.10%	0.00%	0.00	3.50%	1.90%	0.75%	1.25%	1.05%	35.65%	42.10%	3.40%
The Southern Part	23.27%	29.00%	3.80%	0.00	7.10%	0.33%	4.47%	11.47%	5.47%	5.60%	8.00%	1.53%

Phyllite which showed 61% and 81% heavy mineral ratios respectively.

3-3-2-2 Specific Nature of the Heavy Mineral Ratios in the Southern Part

The heavy mineral ratio of thirty panned samples which collected from the Southern Part are divided into three groups on the basis of its heavy mineral ratio to whole sample. These three groups are distribute in different region as follows:

(A) Group No. 1 (Heavy mineral ratios are 64 to 92%)

This group consists of 21 samples.

The component minerals are mainly magnetite, chromite and ilmenite. A negative correlation is noted between the magnetite and chromite ratios. Ilmenite ratio shows a considerable range.

The group No. 1 samples are observed at the surrounding area of the ultramafic rocks which are locate from Mt. Beaufort to the Central Range in the central southern part of the main Palawan Island and from Pulute Range to Mt. Mantalibgajan in the southern part of the main Palawan Island.

The abovementioned areas correspond to ultramafic rock and Cretaceous basalt distributed areas.

(B) Group No. 2 (Heavy mineral ratios are 41 to 53%)

This group consists of 5 samples.

The component minerals are mainly magnetite, chromite and ilmenite. Close negative correlations are exhibited between magnetite and chromite, chromite and ilmenite, while positive correlation is exhibited between magnetite and ilmenite.

The group No. 2 samples are observed only at restricted areas at the surrounding part of the ophiolitic rocks which are distributed from End Peak to Mt. Calatugas in the central southern part of main Palawan Island.

The country rocks of these samples are; two were taken from the San Vicente Gabbro; two from Mt. Beaufort Ultramafics and one from the Espina Basalt.

(C) Group No. 3 (Heavy mineral ratio are 5 to 21%)

This group consists of 4 samples.

The correlation is unclear due to the low heavy mineral ratios and the small number of samples.

This group of samples are observed at the southwestern part of the main Palawan Island which corresponds to the transition point between the mountain range and the alluvial fan. Such places used to be composed of various kinds of sediments which is considered to be the cause of the low contents of the heavy mineral contents noted were not high.

Table-24 Correlaion Coefficients of Constituent Minerals of Panned Samples (Northern Part)

	mt	cm	il	ru	Fe	Z	ol	P	Ho	F	Q	oth
mt	1.00											
cm	0.88	1.00										
il	–	–	1.00									
ru	–	–	–	1.00								
Fe	0.47	0.44	–	–	1.00							
Z	0.40	0.43	–	–	0.79	1.00						
ol	0.71	0.56	–	–	0.55	0.44	1.00					
P	0.46	0.35	–	–	0.35	0.09	0.83	1.00				
Ho	−0.26	−0.22	–	–	−0.26	−0.14	0.01	0.22	1.00			
F	−0.39	−0.39	–	–	−0.36	−0.32	−0.51	−0.50	−0.11	1.00		
Q	−0.36	−0.36	–	–	−0.23	−0.24	−0.12	0.08	0.28	−0.65	1.00	
oth	0.35	−0.03	–	–	0.28	0.06	0.58	0.63	−0.10	−0.32	0.13	1.00

Table-25 Correlaion Coefficients of Constituent Minerals of Panned Samples (Southern Part)

	mt	cm	il	ru	Fe	Z	ol	P	Ho	F	Q	oth
mt	1.00											
cm	−0.28	1.00										
il	0.31	0.06	1.00									
ru	–	–	–	1.00								
Fe	−0.16	0.19	−0.11	–	1.00							
Z	0.16	−0.11	−0.04	–	0.23	1.00						
ol	−0.30	0.12	−0.20	–	0.36	0.50	1.00					
P	−0.16	−0.45	−0.20	–	−0.21	−0.10	0.01	1.00				
Ho	−0.30	−0.40	−0.20	–	−0.17	−0.09	−0.09	0.21	1.00			
F	−0.51	0.13	−0.30	–	−0.14	−0.08	0.30	0.23	0.00	1.00		
Q	−0.28	−0.41	10.20	–	−0.14	−0.14	−0.24	0.02	−0.01	0.06	1.00	
oth	−0.31	−0.25	−0.26	–	−0.17	−0.17	0.09	0.10	0.88	−0.07	−0.06	1.00

4. Correlation with the Existing Regional Data

The compilation of the aeromagnetic map and the extraction of the lineaments form the LANDSAT image analyses and the gravimetric map were carried out during the first phase (1984) of the project.

These data, as presented in this report, were plotted on 1:1,000,000 scale topographic maps (Attached Plates-5 to -7) and were analysed in term of their significance and relationship with the results of the survey works.

4-1 Aeromagnetic Data (Attached Plate 6-1 ~ 6-2)

The available aeromagnetic survey data covered the Northern most part of the Palawan Island and the Calamian Islands Group. The survey was conducted utilizing an airborne proton magnetometer. Flight operations involved coverage of N-S traverse lines spaced at 2.5 km and E-W tie lines spaced at 10 km at an altitude of 6,000 barometric feet. The results have been compiled as IGRF Map (The International Geomagnetic Reference Field Map).

An examination of this map shows that the NE-SW trend of isomagnetic contour lines have a tendency to be higher in the NW and lower in the SE part. The trend is the same as that of the general strike of the Paleozoic to Mesozoic Formations which underlie the covered area.

From the observed tendency is inferred that the thickness of the above mentioned formations which have low magnetic susceptibilities nature is increasing towards the SE and decreasing towards the NW side.

4-2 Lineament Data (Attached Plate 7-1 ~ 7-2)

Parallel LANDSAT image analyses were carried out by JICA-MMAJ and the Philippine government counterpart in 1985.

Attached Plate-7 combines these two linaement data sources using different colors.

The relationships between the geological structures of each region and these lineaments are as follows

1) In Busuanga Island anticlinorium structures and the axial planes are reflected by the lineaments.

2) In the Northern Palawan Area, N-S and NE-SW directed thrusts and complicated structures of the metamorphosed formations are indicated by the lineaments.

3) In the Southern Palawan Area, many NE-SW lineaments which reflecting the trends of the thrusts are observed.

4-3 Gravity Data (Attached Plate 5-2)

In the Palawan Area, the gravity data (Bouguer anomaly) is available only for the Balabac Island. From this map, a remarkable high anomaly is observed at the central part of Balabac Peak in the east coast. The high anomaly is located near the Cretaceous Espina basalt, so this anomaly is inferred to indicate high density basaltic rock.

5. The Relationships between the Mineral Showings and the Geochemical Anomalies

The relationships between the mineral showings and the geochemical anomalies are shown in Table-26.

According to this table, on the univariate analyses, Mn mineral showings are closely accompanied by Mn, Cu and Sb anomalous cells, Cr mineral showings are closely associated with Cr, Zn, Mn, Ni, Co anomalous cells and massive sulphide mineral showings are closely accompanied by Cu, Zn, As, Mn and Hg anomalous cells. On the multivariate analysis, Mn mineral showings are associated with Factor No. 1 (after rotation) and Factor No. 3 (after rotation), nickel laterite mineral showings are associated with Factor No. 2 (before rotation) and Factor No. 3 (before and after rotation) while massive sulphide mineral showings are closely reflected by Factor No. 2 (before rotation) and Factor No. 3 (before rotation).

Table-26 Relationship between Mineral Showings and Geochemical Anomalies

	Index No.	Mineral Showings Name	Commodity	Cell Average Analysis														Highpass Filter Analysis														Factor Analysis				
				Cu	Pb	Zn	Ag	As	Mn	Ni	Co	Mo	Hg	Cr	Sb	Sn	W	Cu	Pb	Zn	Ag	As	Mn	Ni	Co	Mo	Hg	Cr	Sb	Sn	W	No.1	No.2	No. 3		No.4
Northpearrnt	4	Kabol-Kabol	Mn	–	–	–	–	–	–	–	–	–	○	○	–	–	–	–	–	–	–	–	–	–	–	–	–	–	–	–	–	Post –	Pre –	Pre	Post ◎	Pre –
	64	Lanka	Mn	–	–	–	–	–	◎	–	○	–	–	–	–	–	–	–	–	–	–	–	–	–	–	–	–	–	–	–	◎	–		–	–
	65	Dapdapan	Mn	◎	–	–	–	◎	◎	–	○	–	○	–	◎	–	–	–	–	–	–	–	○	–	–	–	–	○	○	–	–	◎	–		–	–
	66	Paly Is.	Cr	–	–	◎	–	–	◎	◎	◎	–	–	◎	–	–	–	–	–	–	–	–	–	–	–	–	–	–	–	–	–	◎	○		–	–
Southern Part	26	Atlas Mine	Cr	–	–	◎	–	–	◎	◎	◎		–	◎				○	–	◎	–	–	○	◎	◎		–	○				Pre ◎	Pre –	Pre –	Post –	
	39	Pulute Range	Ni	○	–	–	–	–	–	–	–		–	–				–	–	–	–	–	–	–	–		–	–				–	◎	–	–	
	54	Rio Tuba	Ni	–	–	◎	–	–	◎	◎	◎		–	–				–	–	–	–	–	–	–	–		–	–				–	◎	◎	◎	
	56	Balabac	Cu	–	–	○	–	○	○	–	–		–	–				–	–	–	–	–	–	–	–		–	–				–	◎		◎	
	62	Berong	Cr	–	–	◎	–	–	◎	◎	◎		–	◎				–	–	◎	–	–	○	○	◎		○	–				◎	–		–	
	67	Richman	Cr	–	–	–	–	–	○	○	○		–	◎				○	–	–	–	–	–	○	○		–	○				◎	–		–	
	68	Boyo	Cr	–	–	–	–	–	–	–	–		–	–				–	–	–	–	–	–	–	–		–	–				–	–		–	
	69	Benguet	Cr	○	–	–	–	–	–	–	–		–	–				–	–	–	–	–	–	–	–		–	–				–	–		–	
	70	Romarao	Cr	–	–	◎	–	–	◎	◎	◎		–	◎				–	–	○	–	–	○	○	○		–	–				◎	–		–	
	71	Ibatong	Ni	–	–	–	–	–	○	○	○		–	–				–	–	–	–	–	–	–	–		–	–				◎	–		–	
	72	Malasgao	Ni	–	–	–	–	–	○	○	◎		–	◎				–	–	–	–	–	–	–	–		–	○				◎	○		–	
	73	Bethlehem	Ni	–	–	–	–	–	○	◎	◎		–	◎				–	–	–	–	–	○	◎	◎		–	○				◎			–	
	74	Bethlehem west	Ni	–	–	–	–	–	○	○	◎		–	○				–	–	–	–	–	–	○	–		–	○				◎	○		–	
	75	Olympic	Ni, Cr	–	–	–	–	○	○	◎	◎		–	○				–	–	–	–	–	–	–	○		–	–				○	◎	◎	–	
	76	Santa Monica	Ni	–	–	–	–	–	○	◎	◎		–	○				–	–	–	–	–	○	–	○		–	–				◎	◎	◎	–	
	77	Trident	Cr	–	–	–	–	–	○	○	◎		–	◎				–	–	–	–	–	–	–	○		–	○				◎	○	◎	–	
	78-80	Barong Barong	Cu	◎	◎	◎	–	○	◎	○	–		○	–				–	–	–	–	–	–	–	–		–	–				◎	◎	◎	–	
	81	Males	Cu	–	–	–	–	–	○	–	○		◎	–				–	–	–	–	○	○	◎	–		–	○				–	–		◎	
	82	Pulot	Cu	○	–	–	–	◎	–	–	○		–	○				–	–	–	–	–	–	–	–		○	–				–	◎		–	

◎ : located in the cell which has over $\overline{X}+1.5\sigma$
○ : located in the cell which has between $\overline{X}+1.0\sigma \sim \overline{X}+1.5\sigma$
– : located in the cell which has below $\overline{X}+1.0\sigma$
Pre : concerned the factor before rotation
Post : concerned the factor after rotation

6. Conclusion

6-1 Consolidated Evaluation of the Survey Results

6-1-1 Geology and Structures

The Palawan area is divided into the Northern Part and the Southern Part by the Sabang Thrust which passes at the east side of Uluagan Bay in the central part of the main Palawan Island. Following this division, analyses and description for each part are carried out.

6-1-1-1 The Northern Part

The Northern Part is composed of the northern part of the main Palawan Island and the Calamian Islands Group. The northeastern portion of this parts is located at the southern end of Manila Trench and forms a stable uplifted terrane.

The northeastern portion is composed mainly of the Paleozoic and Mesozoic chert and limestone formations which are inferred to have been derive from the southern margin of mainland China and drifted southward following the movement of the oceanic plate consequent to the formation of the Southern China Sea. This microcontinental terrane is believed to have collided with the Proto-Philippine arc during Middle Miocene time. (Taylor and Hayes, 1980.)

The southwestern area of the Northern Part is composed mainly of phyllitic and schistose rocks which were Presumed to be formed within dated as Carboniferous to Permian Epoch. The turbidities dated as Cretaceous and Paleogene are distributed at the northwestern area of this part.

The structures of the Northern Part is considerably affected by the collision, as shown by the NW to SE trending anticlinorium formed in the formations of the northeastern area and by the numalous thrusts formed in the southwestern area.

As for the igneous activities in the Northern Part, the Kapoas Diorite intrusion in the west side and the Manguao volcanics in the east side are significant. The former is dated Eocene to Early Oligocene (UNDP, 1984. JICA-MMAJ, 1987) while the latter is estimated as Pleistocene in age.

6-1-1-2 The Souther Part

The Southern Part is the area south of the Sabang thrust the southern part of the main Palawan Island and the Balabac Island. the oldest formation in this part is composed of Cretaceous sedimentary rocks and basalt flows which is overlain unconformably by Paleogene turbiditic sediments.

The ophiolitic rocks derived from the Proto-Sulu-Sea were thrusted over these formations and the major fraction of the central mountain range is made up of these ophiolite units. The Sabang Thrust was also formed at this time which is estimated to be most active from Oligocene until the Miocene.

The Neogene formation overlie and enclose in part of the ophiolite units.

6-1-2 Mineralizations

6-1-2-1 Mineralizations of the Northern Part

The mineral showings investigated in the Northern Part are: Pre-Tertially strata-bound manganese mineral showings in chert at the eastern and central parts of Busuanga Island, vein type manganese mineral showing associated calcite veins at northwestern Culion Island and orthomagmatic dissemination chromite mineral showing at Paly Island, offshore Northern main Palawan island. In addition to the abovementioned mineral showings, an antimony-bearing quartz vein showing at the northwestern area of Tinitian is reported.

The distribution of geochemical anomalies seems to suggest that the Sn, Cu and Zn mineralization in the northeastern main Palawan Island which is inferred to be associated with the Kapoas Diorite.

Table-27 Relation between selected anomalous zones and Results of Geochemical Analyses

	No.	Anomalous Zone	Location	Cell average Analysis											High-pass Filter Analysis											Factor Analysis				Geology and Mineralization
				Cu	Pb	Zn	Ag	As	Mn	Ni	Co	Hg	Cr	Sb	Cu	Pb	Zn	Ag	As	Mn	Ni	Co	Hg	Cr	Sb	1.	2.	3.	4.	
NORTH	1	Eastern part of Busuanga	120° 16′ E 12° 05′ N	○		○		○	○	○	○	○	○	○	○	○	○		○	○	○	○	○	○	○	○				Near the strata bound manganese showing
	2	Eastern part of El Nido	119° 30′ E 11° 15′ N			○		○	○		○					○	○		○				○			○		○	○	Near the stock of Kapoas diorite
	3	Northwestern of Pancol	119° 20′ E 10° 58′ N	○		○		○	○	○	○	○					○		○			○	○	○	○	○		○	○	ditto
	4	Northwestern of Tinitian	119° 08′ E 10° 07′ N					○						○					○						○			○		Near the Sb showing
SOUTH	5	North of Puerto Pricesa	118° 40′ E 9° 55′ N	○		○			○	○	○	○	○			○	○						○				○	○		Hydrothermal vein in Cretaceous unit
	6	Long Point in western coast to Panacan in eastern coast	118° 20′ E 9° 30′ N			○		○	○	○	○	○	○			○	○		○	○	○	○	○	○		○	○			Several lenticular chromite showings associated with dunite
	7	Surrounded part of southwest mountaine range	117° 52′ E 9° 52′ N	○	○	○		○	○	○	○	○				○				○	○	○					○	○		Lenticular chromite, nickel laterite and Cyprus type copper showings distributed
	8	Southwest of Rio Tuba	117° 25′ E 8° 34′ N	○		○		○	○	○	○					○	○		○	○	○					○	○	○		Nickel laterite and Cyprus type copper showings are observed
	9	East side of Balabas Is.	117° 04′ E 7° 54′ N	○		○		○	○																		○	○		Cu, Zn and As anomalies at south side of mined area

○ : Concerned elements to anomalous zone.

6-1-2-2 Mineralization of the Souther Part

The mineral showings which were investigated in the Southern Part consist of the following: Orthomagmatic lenticular chromite mineral showings, nickel-laterite mineral showings, Cyprus type massive sulphide mineral showings and hydrothermal vein type mineral showings.In addition to the above mentioned, the vein type mercury mineralization is known at the northern part of Puerto Princesa in central main Palawan Island.

The distribution of geochemical anomalies also indicated Cu, Zn and Hg mineralizations at the north of Puerto Princesa in the central part of the main Palawan Island.

6-1-3 Synthetic Evaluation of the Results of Geochemical Analyses

Anomalous zones are selected from anomalous cells which are defined by geochemical analysis methods utilizing the following standards.

(A) Each anomalous zone should more or less be defined by over two detected element anomalous values.

(B) Each anomalous zone should at least be suggested over two methods of geochemical analyses.

Table-27 shows the anomalous zones selected based on the above standards and features of each anomalous zone.

Evaluation of the Anomalous Zones in the Palawan Area. (Zone No. corresponds to that of Table-27) and mineral showings No. corresponds to that of Table-1 and Table-2).

No. 1; Eastern Part of Busuanga Island:

This zone has overlapping anomalies of various elements. Aside from stratified manganese mineralization, no other mineral showing, alternation zone nor igneous activity is observed. Thus, those anomalies are inferred to have been derived from some other mechanism besides mineralization (for example; absorption of pelitic sediments. (Footnote 1). Therefore, this zone is excluded from the promising zone

No. 2; Eastern part of El Nido,

No. 3; Northwestern Part of Pancol:

These zones are located around the Kapoas Diorite intrusion area. Mineral showing is unknown but the combination of anomalous elements suggests that these anomalous values are probably derived from the mineralization associated with the diorite intrusion. Thus, these zones are selected as low priority promising zones (VI).

No. 4; Northwestern part of Tinitian:

This zone has an antimony mineral showing which was delineated by the UNDP survey. According to that report, stibnite disseminated in argillaceous zone (20 cm width) is observed in the altered Caramay Schist. Thus the anomalous zone of Sb and As is selected as promising zone (V).

No. 5; Northern part of Puerto Princesa:

This zone has overlapping anomalies of various elements. UNDP investigated chromite, copper, mercury and manganese mineral showings (1981 - 1985). Mercury mine was operational in the past and there there are still numerous occurrences observable. Thus, this zone is selected as promising zone (IV).

No. 6; Long Point in western coast to Panacan in eastern coast:

This zone has a wide distribution from Long Point in the west coast to Panacan in the east coast. Cobalt and chromium anomalous zones are almost overlapping within the ultramafic rocks. A promising zone (III) is delineated at the east side of Berong, in which Romarao (70, Cr), Berong (62, Cr) and Ibat-ong (71, Ni) mineral showings are located. (Mineral showing numbers correspond to that of Table-1 and Table-2.)

No. 7; Vicinity of the Mountain Range in the southwestern Palawan:

This zone is confined within the Cretaceous Espina basalt and the Eocene gabbro which is situated along the lower slopes of the central mountain range in the southwestern part of Quezon-Aboabo area. Numerous mineral showings were located within this zone, in Pulute Range (39, Ni), in Barong-Barong A, B and C (78, 79, 80, Cu), Males (81, Cu), and in Pulot (82, Cu). Two promising zones are selected. One is the Pulute Range (39) (I) and the other is Barong- Barong A, B and C (78, 79, 80)(II).

No. 8; Southwestern part of Rio Tuba:

This zone is a long the peripheral areas of the Rio Tuba Mine which is under operation. Thus this zone is excluded from the promising zone.

No. 9; Eastern coast of Balabac Island:

This zone is around the area of the former Balabac Mine. Cu, Zn, As and Mn anomalies are overlapping within the south side of the Balabac Mine. This zone is excluded from the promising zone because the locality is very near a closed mine.

6-2 Conclusions

The order of priority of the exploration promising areas mentioned above are as follows:

(I) Overlapping anomalous zones of Cu, Mn, Ni and Co at the Pulute Range in the southwestern part of the main Palawan Island: Cretaceous formations and overthrusted ultramafic rocks are distributed in this area. Nickel laterite mineral showing is know. Assumed commodities are Ni and Cr which are associated with the Cretaceous formations. (In the Southern Part)

(II) The surrounding area of Barong-Barong mineral showings: The Cretaceous Espina Basalt is distributed in this area. Copper mineral showings of Cyprus type massive sulphides are

---

Footnote 1: In the example, absorption of heavy metal element in pelitic sediments has been reported on stratified Mn deposits in Japan. Hamachi, T. 1962.

known. Assumed commodities are Cu, Pb and Zn. (In the Southern Part)

(III) The eastern part of Berong at the northwestern coast in the central southern part of the main Palawan Island: The ultramafic rocks are distributed in this area. Romarao (70, Cr), Berong (62, Cr), and Ibatong (71, Ni) mineral showings are known. Assumed commodities are Cr and Ni. (In the Southern Part)

(IV) The northern part of Puerto Princesa in the central part of the main Palawan Island: Overthrusted ultramafic rocks and Cretaceous formations which are exposed as inliers under the ultramafics are present in this area. Cr, Cu, Hg and Mn mineral showings are known. Assumed commodities are Hg, Cu and Mn. (In the Southern Part)

(V) The northwestern part of Tinitian at the southeastern coast in the central eastern part of the main Palawan Island: The Caramay Schist is distributed in this area. Antimony mineral showings which accompany quartz veins are known. Assumed commodity is Sb. (In the Northern Part)

(VI) This area extends from El Nido to Kapoas Peninsula in the northwestern part of the main Palawan Island: Several stocks of diorite are observed with a NNE-SSW direction in this area. Cu, Zn and Sn hydrothermal veins which are associated with these diorite stocks are assumed. (In the Northern Part)

References

Bassoullet, J. P., 1983, Jurassic Microfossils from the Philippines: United Nations ESCAP, CCOP Technical Bulletin, vol.16, p.31-38.

Beauvais, L., 1983, Jurassic Cnidaria from the Philippines and Sumatra: United Nations ESCAP, CCOP Technical Bulletin, vol.16, p.39-61.

BMG, 1981, Geology and Mineral Resources of the Philippines, vol.I.

BMG, 1986, Geology and Mineral Resources of the Philippines, vol.II.

BMG-UNDTCD, PHI/85/001, 1985, Geochemical Analysis Procedure No. 1, 2, 4, 5, 6, 8, 9, 11, 13, 14 and 15.

Casasola, A.G., 1954, unpub., Preliminary Report on the Petroleum and Geological Reconnaissance Survey of Southern Palawan: Bureau of Mines, 17p.

David, P. and Fontaine, H., 1982, unpub., Eocene Limestone Offshore Northeast Palawan Island: Bureau of Mines and Geosciences, 9p.

DENR, 1985, Lineament Maps from Landsat Imagery: (Natural Resources Management Center, 1985.)

Fernandez, H., 1968, The Geology of Cinnabar Deposits of Central Palawan: The Philippine Geologist, Manila, vol.22, p.91-105.

Fontaine, H., David, P., Pardede, R. and Suwarna, N., 1983, Marine Jurrasic in Southeast Asia: United Nations ESCAP, CCOP Technical Bulletin, vol.16, p.3-30.

Fontaine, H., David, P. and Tien, N., 198-, unpub., Northwest Panay-South Tablas: A repetition of the geology of North Palawan Area: Bureau of Mines and Geisciences, 8p.

Fontaine, H., 1979, unpub., Preliminary Report on the Geology of the Calamian Islands: Bureau of Mines and Geosciences, Manila.

Friedman, G. M. and Sanders, J. E., 1978, Principles of Sedimentology: John Widely and sons, New York, 792p.

Hamachi, T., 1962, The Uraniferous Pelitic Sediment Closely Related to Manganiferous Ore Deposits in Japan: Japanese Journal of Geology and Geography, vol. XXXIII, Nos.2-4, p.53-72.

Hamburger, M., Cardwell, R. and Isacks, B., 1981, Seismo-tectonics of the Luzon, Philippines Region (Progress Report): Philippine SEATAR Committee, Workshop on the Luzon-Marianas Transect, Manila.

Hashimoto, W., 1981, Contributions to the Geology and Paleontology of Southeast Asia, CCXVIII: Supplementary Notes on the Geological Development of the Philippines by Hashimoto (reprint from Geology and Paleontology of Southeast Asia), Tokyo, vol.22, pp.171-191.

Hashimoto, W., and Sato, T., 1973, Geological Structure of North Palawan and its Bearing on the Geological History of the Philippines: Geology and Paleontology of Southeast Asia, vol.13, p.145-161.

Hinz, K. and Schloter, H. U., 1983, Geology of the Dangerous Grounds, South China Sea and the Continental Margin Off SW Palawan: Results of SONNE cruises SO-23 and SO-27: Bundesanstalt Fur Geowissenschaften and Rohstoffe, Hannover, 17p.

Holloway, N. H., 1982, North Palawan Block, Philippines - Its Relation to Asian Mainland and role in Evolution of South China Sea: The American of Petroleum Geologist Bulletin, vol.66, No.9, p.1355-1383.

Isozaki, Y., Amiscaray, E. A. and Rillon, A.1988, unpub., Permian, Triassic, and Jurassic Bedded Radiolarian Cherts in North Palawan Block Philippines: Evidence of Late Mesozoic Subduction-Accretion: Mines and Geosciences Bureau, Quezon City, 14p.

JICA-MMAJ, 1985, Report on the Mineral Exploration - Mineral Deposits and Tectonics of Two Contrasting Geologic Environments in the Republic of the Philippines, Phase I: Japan 174p.

JICA-MMAJ, 1987, Report on the Mineral Exploration - Mineral Deposits and Tectonics of Two Contrasting Geologic Environments in the Republic of the Philippines, Phase III: Japan 442p.

JICA-MMAJ, 1988, Report on the Mineral Exploration - Mineral Deposits and Tectonics of Two Contrasting Geologic Environments in the Republic of the Philippines, Phase IV: Japan 347p.

John, T. U., 1963, Deposits of Balabac Island, Philippines: The Philippine Geologist, Manila.

Martin, S. G., 1972, unpub., Progress Report on the Petroleum Geological Survey of Southern Palawan: Bureau of Mines 40p.

McCabe, R., Almasco, J. and Diegor, W., 1982, Geologic and Paleomagnetic Evidence for a Possible Miocene Collision in Western Panay, Central Philippines: Geology, vol.10, p.325-329.

McCabe, R., Almasco, J. N. and Jumul, G. P., Jr., 1985, Terranes in the Central Philippines: The Philippine Geologist, Manila, vol.39, No.1, p.3-23.

Mitchell, A. H. G., Hernandez, F. and dela Cruz, A. P., 1985, Cenozoic Evolution of the Philippine Archipelgo: Journal of Southeast Asian Earth Sciences, vol.1, No.1, pp.3-22.

Mitchell, A. H. G., Fstacio, R., Flores, R., Lazo, E., Manuel, E., Salvado, H., and Santiago, A., 1985, Geology of Central Palawan: The Philippine Geologist, vol.39, No.3, p.1-43.

Rammlmair, D., 1985, Chromite in the Philippines: Its Relationship to the tectonic setting of the Host Ophiolite: Example from Zambales and Palawan: Federal Institute for Geosciences and Natural Resources, Hannover, p.285-309.

Rangin, C., Stephen, J. F. and Muller, C., 1980, unpub., Jammed South China Sea-Middle Oligocene Oceanic Crust into Mindoro Collision Zone (Philippines), 27p.

Rillon, A. and Sajona F., 1986, unpub., Geology and Mineral Resources of North Palawan (Mainland).

Salvadivar-Sali, A., Oesterle, H. G. and Brownlee, D. N., 1981, The Geology of Offshore Northwest Palawan, Philippinees: Proceedings of ASCOPE, 1981 (2nd Cont.) p. 99-123.

Salvador, J. and Cruz, E., 1988, unpub., Geology and Mineralization of Busuanga and Culion Islands: RP-Japan Project, Mines and Geosciences Bureau, 27p.

Santos, V. Delos, 1959, Preliminary Report on the Geology and Mineral Resources of Central Palawan: The Philippine Geologist, vol.13, p.104-141.

Santos, R. A. and Santos, E. A., 1986, unpub., Geology of South Central Palawan and Its Tectonic Implications.

Santos, R. A., 1988, ms., The Geology of Palawan and Its Tectonic Implications.

Sunga, V. and Salas, R., 1987, unpub., Geology and Mineralization of South Palawan.

Tamesis, E. V., Manalac, E. V., Reyes, C. A. and Ote, L. M., 1973, Late Tertiary Geologic History of the Continental shelf off Northwestern Palawan, Philippines: Proceedings, Reginal Conference on the Geology of Southeast Asia, 1972: Geological Society of Malaysia, Bulletin, vol. 6, p. 165-176.

Taylor, B., and Hayes, D. E., 1980, The Tectonic Evolution of the South China Sea Basin: The Tectonic and Geologic Evolution of Southeast Asian Seas and Islands. Edited by D. E. Hayes. Geophysical Monograph Series, No.23, p.89-104.

Taylor, B. and Hayes, D. E., 1983, Origin and history of the South China Sea Basin: The Tectonic and Geologic Evolution of Southeast Asian Seas and Islands. Edited by D. E. Hayes. Geophysical Monograph Series, No.27, p.23-56.

Thompson, M. and Hoearth, R. J., 1973, A New Approach to the Estimation of Analytical Precision. Journal of Geochemical Exploration, vol.9, p.23-30.

United Nations, DP/UN/PHI-79-004/6, 1985, Technical Report No.6, Geology of Palawan.

Wolfart, R., 1984, Stratigraphy of Palawan Island, Philippines: Federal Institute for Geosciences and Natural Resources, Hannover, 60p.

---

ms.; manuscript
unpub.; unpublished

PL-1-1　Northern Palawan Geological Map and Section (1/1,000,000)

PL-1-2　Southern Palawan Geological Map and Section (1/1,000,000)

LEGEND

CENOZOIC
- QUATERNARY
  - HOLLOCENE — Qa — Alluvium
  - PLEISTOCENE — Qvb — Manguao volcanics, Aphanitic basalt flow
- TERTIARY
  - PLIOCENE — PLi — Iwahig F. Consist of Pusok conglomerate and Panoyan Ls.
  - ※Melange
  - MIOCENE ~ OLIGOCENE — St. Paul's Ls. Fossiliferous limestone
  - EOCENE — Panas F. Sandstone interbedded with shale and mudstone; Pabellion Ls. Massive crystalline and fossiliferous limestone; Paly Ultramafics Serpentinized harzburgite with some bands of dunite

Kapoas Intrusive

Mt. Beaufort Ultramafics Serpentinized peridotite and dunite

MESOZOIC
- CRETACEOUS — Bonyan Clastics Turbidite formation. Sandstone interbedded with mudstone and conglomerate; Guinlo F. Massive sandstone interbedded with mudstone and conglomerate
- JURASSIC — Busuanga Chert, Red, black, grey chert; Imorgue Ls. Massive to bedded limestone
- TRIASSIC — Liminang Cong Chert. Physically similar to the Busuanga chert, but the radiolarian assemblage is of different age

Coron Ls. Crystalline reefal limestone

Minilog Ls. Massive limestone, partly recrystallized and colitic

PALEOZOIC
- PERMIAN — Bacuit F. Alternation of sandstone and shale. Chert interbedded conglomerate and limestone
- CARBONIFEROUS — Concepcion Phyllite Phyllitic mudstone, shale and sandstone; Caramay Schist Muscovite schist interbedded with quartz mica schist.

Thrust — Normal Fault — Anticline — Syncline

※Melange (The original rocks are referred to be a Cretaceous to Miocene age)

A~A' Section

B~B'~B" Section

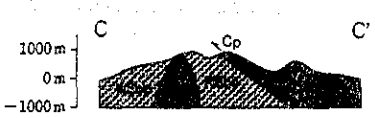

C~C' Section

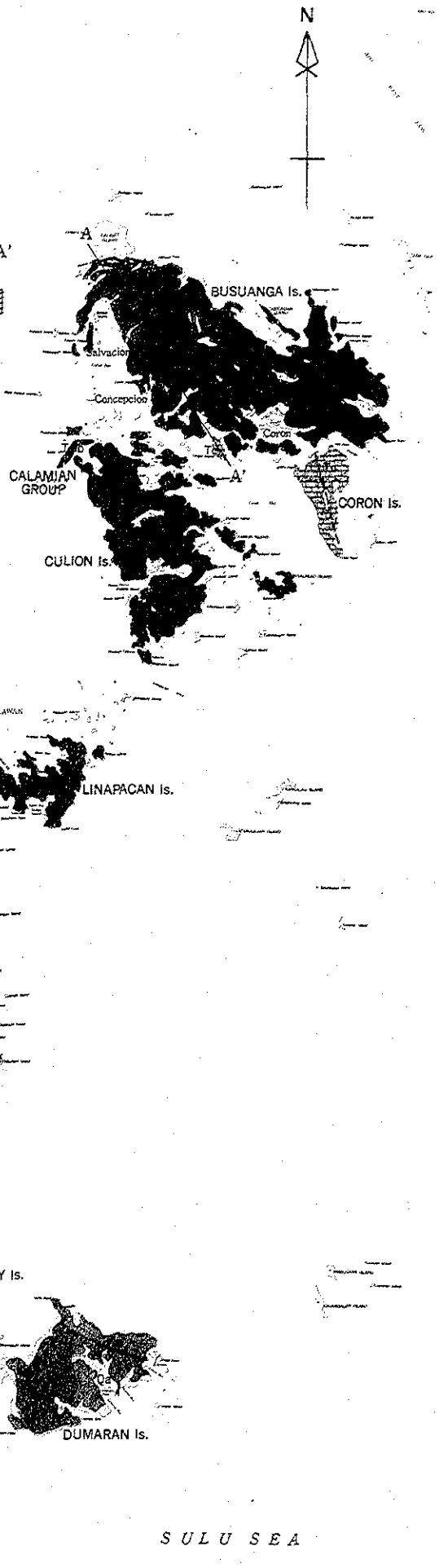

0 10 20 30 40 50km

SCALE 1 : 1,000,000

THE MINERAL EXPLORATION MINERAL DEPOSITS AND TECTONICS OF TWO CONTRASTING GEOLOGIC ENVIRONMENTS IN THE REPUBLIC OF THE PHILIPPINES

CONSOLIDATED REPORT ON NORTHERN PALAWAN

GEOLOGICAL MAP